Journal of Building Engineering 44 (2021) 103425

Contents lists available at ScienceDirect

Journal of Building Engineering

journal homepage: www.elsevier.com/locate/jobe

Porosity-based models for estimating the mechanical properties of self-compacting concrete with coarse and fine recycled concrete aggregate

Víctor Revilla-Cuesta [a,*], Flora Faleschini [b], Mariano A. Zanini [b], Marta Skaf [c], Vanesa Ortega-López [a,b]

[a] Department of Civil Engineering, Escuela Politécnica Superior, University of Burgos, c/ Villadiego s/n, 09001 Burgos, Spain
[b] Department of Civil, Environmental and Architectural Engineering (ICEA), University of Padova, Via Francesco Marzolo 9, 35131 Padova, Italy
[c] Department of Construction, Escuela Politécnica Superior, University of Burgos, c/ Villadiego s/n, 09001 Burgos, Spain

ARTICLE INFO

Keywords:
Recycled concrete aggregate
Self-compacting concrete
Mechanical behavior
Effective capillary porosity
Non-linear multiple regression

ABSTRACT

Predicting the mechanical properties of Self-Compacting Concrete (SCC) containing Recycled Concrete Aggregate (RCA) generally depends, in great part, on the RCA fraction in use. In this study, predictive equations for estimating SCC mechanical properties are developed through SCC porosity indices, so they are applicable to any RCA fraction and amount that may be used. A total of ten SCC mixes were prepared, nine of which containing different proportions of coarse and/or fine RCA (0%, 50% or 100% for both fractions), and the tenth mixed with 100% coarse and fine RCA, and RCA powder 0–1 mm. The following properties were evaluated: compressive strength, modulus of elasticity, splitting tensile strength, flexural strength, and effective porosity as measured with the capillary-water-absorption test. Negative effects on the above properties were recorded for increasing contents of both RCA fractions. The application of simple regression models yielded porosity-based estimations of the mechanical properties of the SCC with an accuracy margin of ±20%, regardless of the RCA fraction and amount. The results of the multiple regression models with compressive strength as a secondary predictive variable presented even greater robustness with accuracy margins of ±10% and almost no significant effect of accidental porosity variations on prediction accuracy. Furthermore, porosity predictions using the 24-h effective water also yielded accurate estimations of all the above mechanical properties. Finally, comparisons with the results of other studies validated the reliability of the models and their accuracy, especially the minimum expected values at a 95% confidence level, at all times lower than the experimental results.

1. Introduction

Concrete consists of cement mixed with water, aggregate, and at times one or more admixtures. Any air that is not released as concrete sets remains occluded within the concrete matrix [1]. Moreover, the delayed reaction between water and cement and water evaporation during the setting process results in the appearance of small pockets of air within the concrete mass, which were previously saturated with water [2]. Both aspects explain why concrete is a porous material, despite its hardened-state robustness [3].

Over recent years, various methods have been developed for accurate evaluation of concrete porosity. On the one hand, computerized axial tomography scanning (CT scan) of specimens can determine pore sizes of up to 100–200 μm in diameter [4]. However, continuous improvement of CT scanning technology has resulted in micro-computed tomography (μCT scan) of higher resolution that now detect smaller pore sizes and, therefore, more accurate estimations of concrete porosity [5]. On the other hand, mercury-intrusion-porosimetry testing can also be used to evaluate concrete porosity, through an analysis of mercury penetration under increasing pressure within the concrete [6]. The sensitivity of mercury intrusion porosimetry is greater than that of μCT scan, in so far as pore sizes of up to 1–5 nm in diameter may be detected, which in turn results in even more accurate estimations of concrete porosity [7]. Nevertheless, the orthodox technique for the evaluation of concrete porosity is the test of capillary water absorption [8]. The slow absorption of water by concrete throughout this test and the low surface tension of water mean that air can be efficiently expelled and the accessible porosity of the concrete can be accurately estimated by differences in weight [1].

* Corresponding author. Department of Civil Engineering, Escuela Politécnica Superior, University of Burgos, c/ Villadiego s/n, 09001 Burgos, Spain.
E-mail addresses: vrevilla@ubu.es (V. Revilla-Cuesta), flora.faleschini@dicea.unipd.it (F. Faleschini), marianoangelo.zanini@dicea.unipd.it (M.A. Zanini), mskaf@ubu.es (M. Skaf), vortega@ubu.es (V. Ortega-López).

https://doi.org/10.1016/j.jobe.2021.103425
Received 3 September 2021; Received in revised form 28 September 2021; Accepted 4 October 2021
Available online 6 October 2021

Acronyms

ANalysis Of VAriance (ANOVA)
Interfacial Transition Zone (ITZ)
Natural Aggregate (NA)
Recycled Concrete Aggregate (RCA)
Self-Compacting Concrete (SCC)
Water-to-Cement (w/c)

Furthermore, no special apparatus is required for the performance of this simple low-cost test [9]. Its disadvantage is that isolated pores that are inaccessible to water cannot be evaluated, which implies slight underestimations of concrete porosity [10].

The development of these techniques accompanies research lines on porosity and the extent to which porosity can be used as an indicator for the estimation of other concrete properties [11]. Firstly, concrete porosity and its variations over time are increasingly studied and observations suggest that it fundamentally evolves during the first 16 h, due to cement hydration, after which porosity remains constant [12]. Secondly, the influence and explanatory power of porosity on concrete durability has also been analyzed [13], as external aggressive agents will penetrate the concrete through the interconnected porous network [10]. Finally, the effects of porosity on concrete and the potential accuracy of porosity as indicator of mechanical properties have been studied because increased porosity levels usually imply worse mechanical behavior. On the one hand, the influence of the Water-to-Cement (w/c) ratio on porosity has been analyzed, as well as its relationship with any other strength-related concrete variable that may be accurately estimated [14]. On the other hand, variations relating to compaction and the fiber content of concrete have been linked to porosity [15], resulting in adequate predictions of the strength behavior of concrete [16]. The results of the literature show that porosity can even explain the fatigue life of concrete [17].

These analyses are nevertheless complex, due to the large number of factors on which the porosity of concrete depends. On the one hand, the mixing process affects porosity and quick mixing will usually lead to increased porosity [13]. On the other hand, the higher the w/c ratio, the higher the porosity, due to the evaporation of larger volumes of water during concrete setting [18]. Furthermore, the use of admixtures can also increase concrete porosity, because of chemical reactions with other components of the concrete mix [19]. The modification of the cement-to-aggregate ratio also alters the interactions between the components, once again varying porosity levels [10]. These aspects mean that individual porosity analyses are necessary whenever the proportion of any concrete component varies or indeed the mixing methods.

Different concrete types have been developed with the above-mentioned modifications to concrete composition described in the previous paragraph [20], leaving each type of concrete with its own porosity patterns [21]. For instance, Self-Compacting Concrete (SCC), characterized by high filling and consistent flowability, needs no vibration during placement [22]. Plasticizer admixtures, ultrafine aggregate, commonly limestone filler, and a low coarse aggregate content are used to reach such high levels of workability [23,24]. Both aspects generally imply higher porosity levels in SCC than in conventional vibrated concrete [25].

A current trend in the construction sector is to increase the sustainability of concrete through the use of alternative aggregates and binders [26–28], which also vary concrete porosity levels and its relationship with other properties of this construction material [29]. Recycled Concrete Aggregate (RCA) consists of crushed concrete elements [30]. The use of both coarse and fine fractions of RCA, in substitution of Natural Aggregate (NA), tends to worsen the mechanical behavior of concrete [31,32], due to three fundamental aspects. First, the possible presence of contaminants in the fine fraction, such as gypsum [33]. In principle, if RCA fines are sourced from faulty concrete components rejected in the precast industry, the presence of such contaminants will be reduced [18]. Secondly, reduced adhesion within the Interfacial Transition Zones (ITZ) is notable, due to adhered mortar [32]. If coarse RCA fractions are used, then that effect is more noticeable [34]. Finally, the resulting increase in porosity due to the worsening interaction and affinity of RCA fractions with cement when compared to NA [35]. Porosity increases are higher when fine RCA is used [36].

Attempts to analyze the effect of RCA on vibrated concrete by studying both coarse and fine fractions have been reported in the literature [37,38]. Furthermore, estimations of the mechanical properties of RCA concrete, in multiple studies, usually depend on the added RCA fraction. First, using the usual procedure to relate compressive strength to the other mechanical properties [31]. Second, by estimating the compressive strength indirectly, using the hammer rebound index [39]. It has even been observed that this property is conditioned by the porosity of the recycled aggregate concrete, underlining the influence of porosity on concrete strength [40]. Thirdly, datasets have been assembled to predict the mechanical behavior of concrete that contains RCA using both Bayesian models [41] and machine learning [42]. Finally, these sorts of predictions have even been based upon numerical simulations [43].

Studies on SCC containing RCA and the prediction of SCC mechanical behavior are much scarcer and are mainly based on the use of compressive strength as a predictive variable [44]. Furthermore, the models that have been developed usually depend on the RCA fraction in use [45]. However, the increased porosity levels following the addition of both RCA fractions may be used to assess and to estimate the mechanical properties of SCC. The aim of this study is therefore to demonstrate that porosity is a magnitude that can be linked to the mechanical behavior of SCC, regardless of the RCA fraction in use and the amounts of RCA that are added. The main novelty demonstrated in this research work is that the mechanical behavior of recycled aggregate SCC can be correlated with its porosity levels through accurate simple-regression and multiple-regression mathematical models, regardless of the RCA fraction used and its amount in the SCC mix. This aspect applied to SCC is novel in the literature. Furthermore, it will be demonstrated in this study that porosity can be estimated according to the SCC mix composition.

Ten SCC mixes of similar flowability were prepared, incorporating 0%, 50% and 100% coarse and/or fine RCA. One of the 100% mixes also included RCA powder. In all the mixtures, in addition to slump flow and viscosity, the most relevant mechanical properties were measured: 7-day and 28-day compressive strength, modulus of elasticity at 7 and 28 days, 28-day splitting tensile strength, and 28-day flexural strength. Moreover, the porosity of all the mixtures was determined through the capillary-water-absorption test. Finally, the relationship between all the mechanical properties and porosity was analyzed in detail, through accurate simple- and multiple-regression statistical models for porosity-based estimations of the mechanical behavior of SCC containing RCA, regardless of the fraction and the amount of added RCA. An accurate estimation of the mechanical behavior of SCC with RCA is essential for the design and construction of real building structures that contain this type of concrete [46].

2. Materials and methods

2.1. Materials

All the mixes were prepared with ordinary Portland cement (CEM I 52.5 R), as per EN 197–1 [47], with a specific gravity of around 3.1 Mg/m^3, and mains water. In addition, two admixtures were added: a plasticizer and a setting regulator. Their purpose was to increase the flowability of the SCC and to reduce the water content required for

adequate self-compactability [37].

Both coarse (4–12 mm) and fine (0–4 mm) fractions of siliceous NA of a rounded shape were used, suitably sized for an appropriate SCC mix. Their density and water absorption levels in 24 h and 15 min (Table 1) represented common values [23,48]. However, as shown in Fig. 1, the fine fraction showed an insufficient fines content to achieve optimum self-compactability. For this reason, limestone powder 0–1 mm, a material commonly used to manufacture mortars [49], was also added to SCC. Likewise, its main physical properties and particle gradation are respectively shown in Table 1 and in Fig. 1.

In the sample mixes of this study, both coarse and fine RCA were used in substitution of 50% and 100% coarse and fine NA. The RCA was from crushed concrete from defective precast components with a minimum compressive strength of 45 MPa, rejected immediately after their manufacture. For one of the mixes, the RCA was ground and sieved to obtain RCA powder (0–1 mm) that replaced limestone powder. The density of the RCA was lower than that of NA, while its water absorption was notably higher regardless of the time period (Table 1) [48]. The RCA showed a continuous particle gradation, suitable for the production of concrete and similar to that of NA (Fig. 1). The RCA fine fraction had a higher fines content than the fine siliceous NA.

2.2. Mix design

In total, 10 mixes were prepared to evaluate the performance of all possible combinations of coarse and fine RCA. The mix-design process was sequential:

- Initially, the reference mix was produced with 0% coarse and fine RCA (100% coarse and fine siliceous NA). The proportions of the different components were initially set according to the specifications of Eurocode 2 [50], although those values were then empirically adjusted to achieve an adequate slump flow of around 750 mm. Cement and water were added in standard amounts for a conventional SCC composition.
- Afterwards, 50% or 100% coarse and/or fine siliceous NA was replaced with RCA of the same fraction by volume correction. The replacement percentages were defined in accordance with the conclusions of a previous study by the authors [34], in which three RCA contents with a similar statistical effect on the mechanical behavior of SCC were detected: 0–25%, 50% and 75–100%.
- Finally, in the mix with 100% coarse and fine RCA, limestone powder was replaced with RCA 0–1 mm. The objective was to study the behavior of a mix made with full RCA replacement of all aggregate fractions.

In all the mixtures, the water content was adjusted according to water absorption of the aggregate within 15 min (Table 1), *i.e.*, the duration of the mixing process. Therefore, the water content was increased when RCA, with higher water absorption levels than NA, was added [45]. In this way, a constant effective w/c ratio (value of 0.50) could be maintained and, in turn, a slump flow between 700 mm and 800 mm in all the mixes. Thus, it was ensured that water content had little or no effect on the results and the effect of the RCA additions could be precisely studied [51].

The mix composition is depicted in Table 2, and, as an example, the joint particle gradation of the mixes produced with 50% coarse RCA and variable amounts of fine RCA is shown in Fig. 2. The correct fit of the

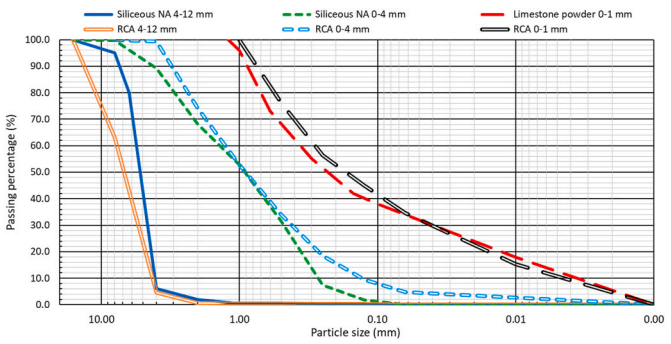

Fig. 1. Particle gradation of the aggregates.

mixes to the Fuller curve may be noted with regard to the proportion of particles smaller than 0.25 mm, thus guaranteeing adequate self-compactability [29]. The mixtures were labelled *"XCYF"*, where *X* and *Y* represented the percentage of coarse and fine RCA additions, respectively (0%, 50% and 100%). The letters *C* and *F* after the amounts referred to the coarse (*C*) and the fine (*F*) fractions of RCA. The mixture incorporating RCA powder 0–1 mm was coded with an *R* at the end.

2.3. Mixing process

A staged mixing process was conducted to maximize SCC flowability and to ensure an adequate level of porosity in all mixtures [52], since rapid mixing generally increases the capillary porosity of the cementitious matrix [13]. This mixing process consisted of three stages, so that different SCC components were added at each stage, as detailed in Fig. 3. After each stage, the SCC was mixed and left to rest for three and 2 min, respectively. Mixing and resting times that after several experimental trials were found to maximize SCC flowability.

2.4. Experimental tests

Once the mixing process had been completed, the slump-flow test (EN 12350–8 [47]) was performed to determine both slump flow and viscosity t_{500}. The slump flow of all the mixes had to be 750 ± 50 mm, to ensure that the mix water had no influence on the results, so that the effect of RCA could be clearly analyzed [51]. Subsequently, the specimens for all the hardened-state tests were prepared. The results of each property were determined through the values obtained from two different specimens. The specimens produced for each mix were as follows:

- Eight 100 × 200-mm cylindrical specimens to measure compressive strength (EN 12390–3 [47]) and modulus of elasticity (12,390–13 [47]) at 7 and at 28 days, as well as the 28-day splitting tensile strength (EN 12390–6 [47]).
- Two 75 × 75 × 275-mm prismatic specimens for measuring flexural strength at 28 days (EN 12390–5 [47]).
- Two 100 × 100 × 100-mm cubic specimens for the capillary-water-absorption test as per RILEM CPC 11.2 [53]. Performed at 28 days, this test was used to estimate the accessible porosity of the mixtures, which was subsequently used to predict their mechanical properties. The capillary-water-absorption test was used to measure SCC porosity, because it is simple and inexpensive to implement. Other

Table 1
Physical properties of aggregates.

	Siliceous NA 4–12 mm	Siliceous NA 0–4 mm	Limestone powder 0–1 mm	RCA 4–12 mm	RCA 0–4 mm	RCA 0–1 mm
Saturated-surface-dry density (Mg/m^3)	2.61	2.57	2.61	2.43	2.38	2.36
24-h water absorption (% wt.)	0.84	0.25	0.53	6.25	7.36	7.47
15-min water absorption (% wt.)	0.71	0.18	0.38	4.90	5.77	6.26

Table 2
Mix composition (kg per cubic meter).

SCC mix	Cement	Water	Coarse NA # RCA	Fine NA # RCA	Limestone # RCA powder	Plasticizer	Setting regulator
0C0F	300	160	580 # 0	940 # 0	340 # 0	4.50	2.20
0C50F	300	180	580 # 0	470 # 435	340 # 0	4.50	2.20
0C100F	300	205	580 # 0	0 # 870	340 # 0	4.50	2.20
50C0F	300	170	290 # 270	940 # 0	340 # 0	4.50	2.20
50C50F	300	195	290 # 270	470 # 435	340 # 0	4.50	2.20
50C100F	300	215	290 # 270	0 # 870	340 # 0	4.50	2.20
100C0F	300	180	0 # 540	940 # 0	340 # 0	4.50	2.20
100C50F	300	205	0 # 540	470 # 435	340 # 0	4.50	2.20
100C100F	300	230	0 # 540	0 # 870	340 # 0	4.50	2.20
100C100FR	300	245	0 # 540	0 # 870	0 # 305	4.50	2.20

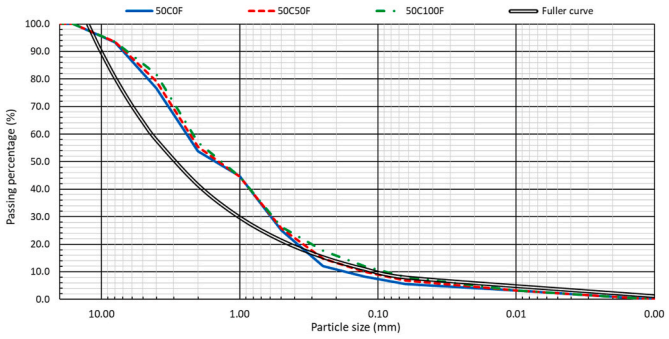

Fig. 2. Joint particle gradation of the SCC mixes.

procedures, such as the CT scan or the mercury-intrusion-porosimetry test, require specific high-cost equipment operated by specialized technical personnel, which cannot be used to measure concrete porosity everywhere in a simple and inexpensive way. The use of such tests might have reduced the practical and easy application of the porosity-based models under development [9].

3. Results and discussion

3.1. Slump flow and viscosity

The slump flow and the viscosity t_{500} of all mixes were measured immediately after the mixing process. In this way, the capability of the SCC mixes to fill the formwork and the speed at which filling was performed could be evaluated [45]. Table 3 shows the slump flow and viscosity t_{500} of the mixtures to an accuracy of ±5 mm and ±0.2 s, respectively. In addition, the percentage variations of both properties when adding coarse and/or fine RCA is also shown.

Since the effective w/c ratio was always equal to 0.50, all the mixes presented a slump flow between 700 and 800 mm (Table 3), the objective defined in the mix design. Thus, the values of all hardened properties were comparable and only the effect of the different RCA fractions was analyzed [51]:

- Coarse RCA caused a minimal decrease in slump flow, always less than 3%, regardless of its content. However, it significantly increased viscosity t_{500} (by around 20%) especially when 100% RCA was added, which can be explained by the irregular shaped RCA particles that enhanced friction between the SCC components [54].
- The use of fine RCA increased the slump flow by 1–6%. The negative effect of its irregular shape was balanced by its higher fines content than siliceous NA (Fig. 1) [55]. Nevertheless, the irregular shaped particles worsened viscosity, which increased by around 15–20%, due to higher internal friction between the mix components [54].
- When adding fine RCA, the higher the content of coarse RCA, the lower the slump flow increase, compared to the slump flow of mix 0C0F. Moreover, viscosity increases caused by each RCA fraction were higher when fine and coarse fractions were simultaneously used. It therefore appears that there was some interaction between both RCA fractions, due to the increased friction between the SCC components in both aggregate fractions.
- The more irregular shape of RCA powder 0–1 mm compared to limestone powder 0–1 mm also worsened both slump flow and viscosity.

Nevertheless, the worsening of the in-fresh behavior was lower than other results reported elsewhere in the literature [29,45], which may be explained by the staged mixing process that maximized RCA water absorption and, in turn, SCC flowability [52].

3.2. Mechanical performance

3.2.1. Compressive strength

The main mechanical property of concrete is compressive strength, which was evaluated in the SCC mixes of this study at 7 and 28 days, as shown in Fig. 4. In addition, trend lines regarding the effect of the addition of fine RCA for each coarse RCA content are also shown.

As expected, the addition of any RCA fraction decreased the compressive strength of SCC [32]. Thus, the compressive strength at 28 days of SCC with 100% NA was 55.7 MPa, while it presented a value of 23.7 MPa (57% compressive strength loss) for SCC with 100% coarse and fine RCA, and RCA powder. The decrease in compressive strength caused by coarse RCA was attributed to decreased adhesion within the ITZ, due to the adhered mortar [34] and to the lower strength of this

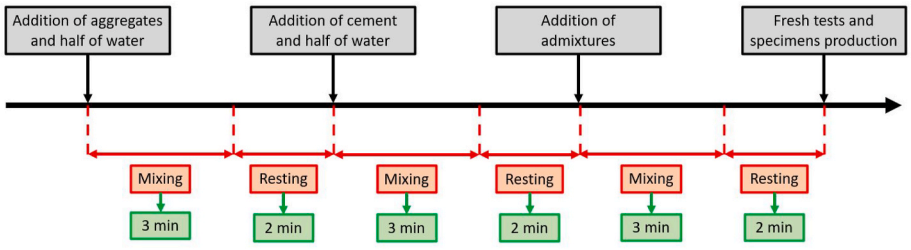

Fig. 3. Mixing process.

Table 3
Slump flow and viscosity t_{500}.

SCC mix	Slump flow (mm)	Viscosity t_{500} (s)	Δ coarse RCA[a] (%)	Δ fine RCA[b] (%)	Δ coarse and fine RCA[c] (%)	Δ RCA powder[d] (%)
0C0F	765	2.6	−/−	−/−	−/−	−/−
0C50F	780	2.6	−/−	+2.0/ 0.0	+2.0/ 0.0	−/−
0C100F	810	3.0	−/−	+5.9/ +15.4	+5.9/ +15.4	−/−
50C0F	765	2.6	0.0/ 0.0	−/−	0.0/0.0	−/−
50C50F	775	2.8	−0.6/ +7.7	+1.3/ +7.7	+1.3/ +7.7	−/−
50C100F	800	3.0	−1.2/ 0.0	+4.6/ +15.4	+4.6/ +15.4	−/−
100C0F	755	3.0	−1.3/ +15.4	−/−	−1.3/ +15.4	−/−
100C50F	760	3.2	−2.6/ +23.1	+0.7/ +6.7	−0.7/ +23.1	−/−
100C100F	800	3.6	−1.2/ +20.0	+6.0/ +20.0	+4.6/ +38.5	−/−
100C100FR	775	4.0	−/−	−/−	−/−	−3.1/ +11.1

[a] Variation of slump flow/viscosity when adding coarse RCA to a mix with the same content of fine RCA and 0% coarse RCA.
[b] Variation of slump flow/viscosity when adding fine RCA to a mix with 0% fine RCA and the same content of coarse RCA.
[c] Variation of slump flow/viscosity regarding the 0C0F mix.
[d] Variation of slump flow/viscosity regarding the 100C100F mix.

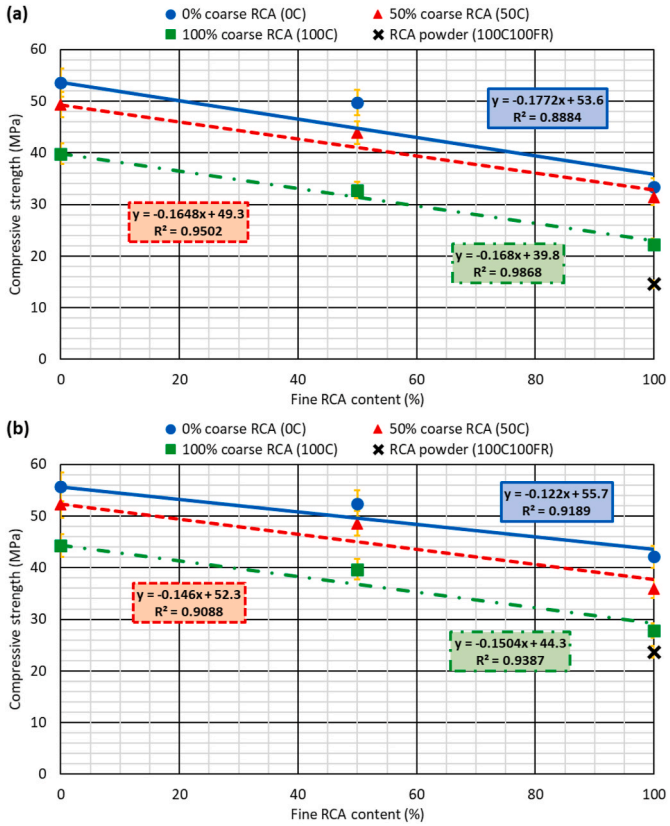

Fig. 4. (a) 7-day compressive strength; (b) 28-day compressive strength.

waste compared to NA [56]. Regarding fine RCA, the presence of altered mortar particles and the increased porosity of the cementitious matrix that it caused (aspect shown in section 3.3) were the most detrimental aspects [57], which led to a higher decrease of compressive strength than coarse RCA, as also shown in other studies [58,59]. The use of RCA powder meant extending the harmful effects of fine RCA to the powder fraction of the aggregate [55], which is necessary to achieve adequate self-compactability, resulting in an even greater decrease in compressive strength.

In absolute values, the compressive strength reduction of SCC with the addition of a specific percentage of coarse RCA was the same regardless of the content of fine RCA. So, the addition of 50% coarse RCA always caused a reduction in the compressive strength at 28 days of 3–5 MPa, and 14–16 MPa for 100% coarse RCA. Similarly, adding a certain amount of fine RCA resulted in a similar loss of compressive strength, regardless of the coarse RCA content of the SCC. A loss that the trend lines with similar slopes at each age reflect in Fig. 4. In fact, the interaction *p*-value between both RCA fractions of the two-way ANOVA, Table 4, was higher than 0.05 (95% confidence level), which demonstrates that the interaction between both RCA fractions was not significant. Thus, it can be stated that the effect of one RCA fraction was not influenced by the added amount of the other RCA fraction. The decrease in compressive strength caused by the simultaneous addition of both fractions was therefore statistically equal to the sum of the decreases separately caused by each fraction [60].

Finally, with regard to the evolution of compressive strength over time, the addition of every RCA fraction delayed the development of compressive strength. The reference mix 0C0F at 7 days had developed 96% of its compressive strength at 28 days, while this value was only 90% and 79% for mixes 100C0F and 0C100F, respectively. Again, fine RCA had the most outstanding negative effect, and no interaction between the two RCA fractions was found (Table 4). The negative effect of RCA powder was far greater, such that the compressive strength at 7 days was only 61% of the 28-day compressive strength. Its behavior might be explained by the higher internal curing of RCA compared to NA, due to its higher water absorption [61], resulting in more noticeably delayed hydration of the cement [62]. This behavior caused that the decrease of compressive strength when adding any RCA fraction was higher at 7 days than at 28 days.

3.2.2. *Modulus of elasticity*

The elastic stiffness of the mixes was defined by determining the modulus of elasticity at 7 and at 28 days, whose values are depicted in Fig. 5. As regards the compressive strength, both RCA fractions reduced

Table 4
Two-way ANOVA of mechanical properties (significant values are those lower than 0.05).

Mechanical property	*p*-Value coarse RCA	*p*-Value fine RCA	*p*-Value interaction coarse and fine RCA
7-day compressive strength	0.0008	0.0003	0.1534
28-day compressive strength	0.0001	0.0001	0.2476
7–28 days compressive strength increase	0.0134	0.0394	0.3598
7-day modulus of elasticity	0.0006	0.0001	0.1756
28-day modulus of elasticity	0.0053	0.0013	0.0976
7–28 days modulus of elasticity increase	0.3532	0.0805	0.5673
28-day splitting tensile strength	0.0005	0.0003	0.0453 [a]
28-day flexural strength	0.0005	0.0004	0.0721

[a] Homogeneous groups: 50C0F and 100C0F; 50C50F and 100C50F; 50C100F and 100C100F.

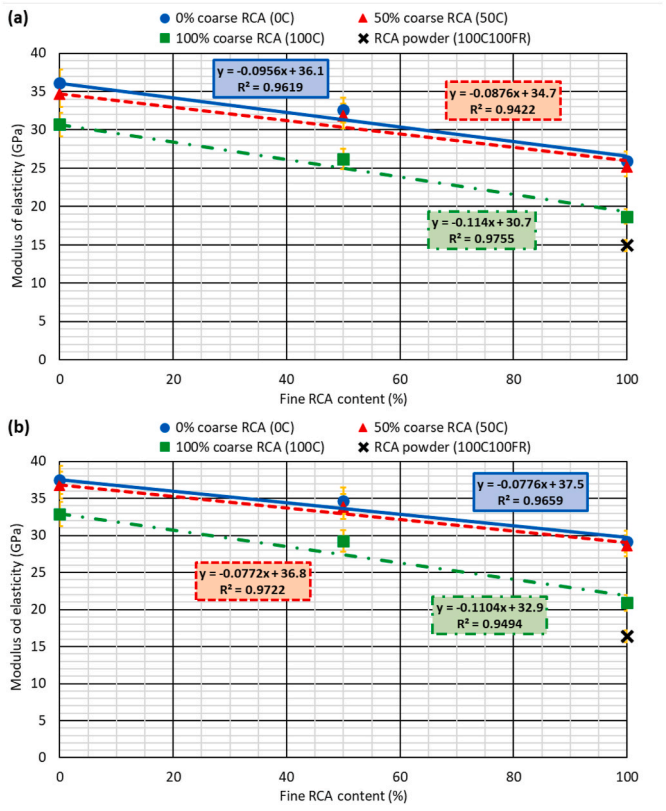

Fig. 5. Modulus of elasticity at (a) 7 days; (b) 28 days.

the modulus of elasticity of the SCC. This decrease at 28 days was 12% when adding 100% coarse RCA, 22% for 100% fine RCA, and 44% for 100% of both RCA fractions. The addition of 50% coarse RCA reduced the modulus of elasticity by around 2% at 28 days, an almost negligible decrease, while 50% fine RCA caused a reduction of 8–10%. Therefore, it is clear that fine RCA had a more detrimental effect than the coarse fraction, although the most notable decrease occurred when adding RCA powder 0–1 mm (56% decrease in mix 100C100FR with respect to mix 0C0F), because this fraction concentrates the most negative effects of the fine fraction 0–4 mm [63]. These decreases are in line with those obtained in other similar studies, in which decreases of 10–15% [59,64] and 20–25% [58,59] were obtained when adding 100% coarse and fine RCA, respectively. None of the RCA fractions affected the development of elastic stiffness over time, as the moduli of elasticity at 7 days of all the mixtures were around 90% of their 28-day moduli of elasticity (two-way ANOVA, Table 4).

The two-way ANOVA values (Table 4) once again showed no interaction between both RCA fractions on the modulus of elasticity of SCC, so that the effects of both RCA fractions were independent of each other. This behavior has also been demonstrated in other similar studies in relation to both vibrated concrete and SCC [31,45]. Alteration of this behavior was only observed in relation to the addition of increasing amounts of fine RCA to SCC with 100% coarse RCA. In these SCC mixes, the use of fine RCA led to a greater decrease in elastic stiffness than in mixes with either 0% or 50% coarse RCA (higher slope of the trend lines). However, this small increase was not enough for that interaction to be significant (p-value less than 0.05).

3.2.3. Splitting tensile strength

The addition of coarse RCA generally decreases adhesion within the ITZ, due to mortar adhering to the NA particles [31]. The application of tensile stress therefore causes detachment between the cementitious matrix and the aggregate instead of the aggregate breaking [65]. The use of fine RCA generally increases these adhesion problems, amplifying the negative effect, as shown by microstructural analyses available in the literature [34]. These two effects mean that the use of any RCA fraction will decrease the splitting tensile strength [59], as observed in this study (Fig. 6). Two relevant aspects can be observed in this figure:

- The decrease in splitting tensile strength with additions of 50% coarse RCA was greater as the fine RCA content increased (6.1% between mixes 0C0F and 50C0F, and 15.8% between mixes 0C100F and 50C100F). This behavior, shown by the trend lines with steeper slopes (Fig. 6), reflects a behavior that was attributed to the increase in adhesion problems when using both RCA fractions simultaneously [34], causing significant interactions between both (two-way ANOVA, Table 4). However, no such behavior was observed between SCC with either 50% or 100% coarse RCA, as any strength decrease was similar regardless of the added amount of fine RCA. Mixtures with 50% and 100% coarse and fine RCA were clustered in homogeneous groups in the two-way ANOVA.
- The mix prepared with 100% RCA in all fractions (100C100FR) showed the worst performance. The RCA powder accentuated the negative effects of the fine RCA (altered mortar particles and increased porosity of the cementitious matrix) and so decreased concrete strength [55,66]. This mix presented a splitting tensile strength of only 1.76 MPa, 58% lower than the strength of mix 0C0F.

3.2.4. Flexural strength

The effect of adding both RCA fractions on the flexural strength of SCC was very similar to the effect on the modulus of elasticity and the compressive strength, as shown in Fig. 7. The following may be mentioned:

- Both RCA fractions worsened the flexural strength of SCC. The addition of 100% of both fractions caused practically the same strength decrease, as both mix 100C0F and mix 0C100F had flexural strengths of 5.2–5.3 MPa, 15% lower than the flexural strength of mix 0C0F. As in other studies on flexural strength, the decreased adhesion within the ITZ, due to the coarse RCA, was as negative as the increased porosity, due to the fine RCA [29].
- No interaction between the two residue fractions was observed, as confirmed by the p-values of the two-way ANOVA (Table 4). Thus, the decrease in flexural strength caused by the addition of any coarse RCA content was very similar, regardless of the fine RCA content of the SCC. On the other hand, the slope of the trend lines reflecting the strength decrease due to fine RCA additions was slightly greater with higher amounts of coarse RCA. However, the underlying strength decrease was of no significance (Table 4), unlike the splitting tensile strength behavior.
- The most damaging fraction for the mechanical behavior of SCC was the RCA powder, as mix 100C100FR presented a flexural strength of

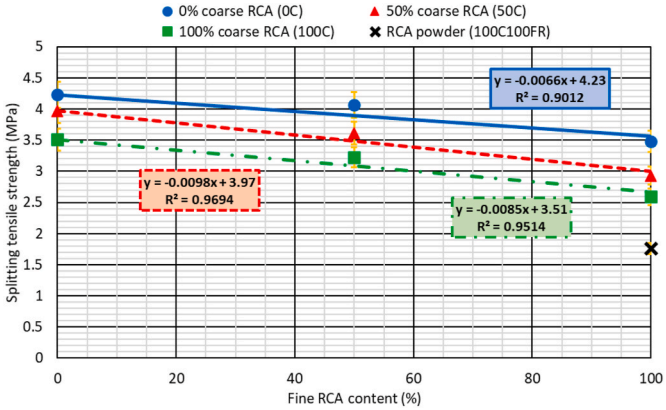

Fig. 6. 28-day splitting tensile strength.

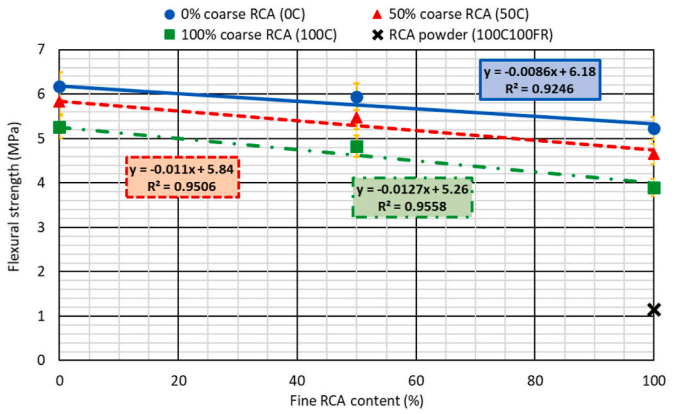

Fig. 7. 28-day flexural strength.

only 1.15 MPa, 70% and 81% lower than the flexural strengths of mixes 100C100F and 0C0F, respectively.

3.2.5. *Statistical significance*

The *p*-values for each factor (coarse RCA content and fine RCA content) and the factorial interaction in the two-way ANalysis Of VAriance (ANOVA) of all the mechanical properties under evaluation are shown in Table 4. The content of both RCA fractions was always significant for mechanical behavior, while the interaction between both RCA fractions was only significant in the splitting tensile strength results. In general, therefore, the decrease of strength/stiffness caused by the simultaneous use of both RCA fractions was statistically equal to the sum of the decreases caused by each individual fraction [44].

3.3. *Capillary-water-absorption test*

The capillary-water-absorption test established the effective porosity of all the mixtures through the determination of concrete capillary water absorption [1]. Unlike other tests to determine porosity, such as the mercury intrusion porosimetry, capillary-water-absorption test is inexpensive and easily performed [9], which is why it was chosen for this study.

3.3.1. *Water absorption*

The measurement of water absorption by capillarity was performed according to RILEM CPC 11.2 [53]. For this purpose, at 28 days, 100 × 100 × 100-mm cubic specimens were prepared in accordance with the humidity specifications as per UNE 83966 [67]. Subsequently, the skin was removed from one of their faces, which was placed in contact with a 5 ± 1 mm layer of water for 72 h, in order for the specimens to absorb water by capillary action. The four lateral faces of the specimens were waterproofed. During the test, the specimens were weighed at different time intervals depending on the time that had elapsed since the beginning of the test. Weighing was performed every hour at the beginning of the test and every 24 h towards the end of the test.

The water absorption levels of the specimens throughout the test (72 h) are shown in Fig. 8. SCC capillary water absorption occurred at a higher rate during the first 6 h of the test, after which it slowed down, as shown by the lower slope of the graph trend lines (Fig. 8). This behavior is standard in concrete: capillary water absorption is very fast at the beginning of the test and it then stabilizes over time, once the pores closest to the absorption surface have been saturated [8,10]. Moreover, the relationship between 72-h water absorption and coarse and/or fine RCA content is shown in Fig. 9, for an easier comparison of water absorption of the mixtures. It can be seen that an increase in the content of either RCA fraction also increased capillary water absorption, as RCA additions need extra water to maintain the flowability of the SCC and an increased w/c ratio raises concrete porosity levels [68], as also do the

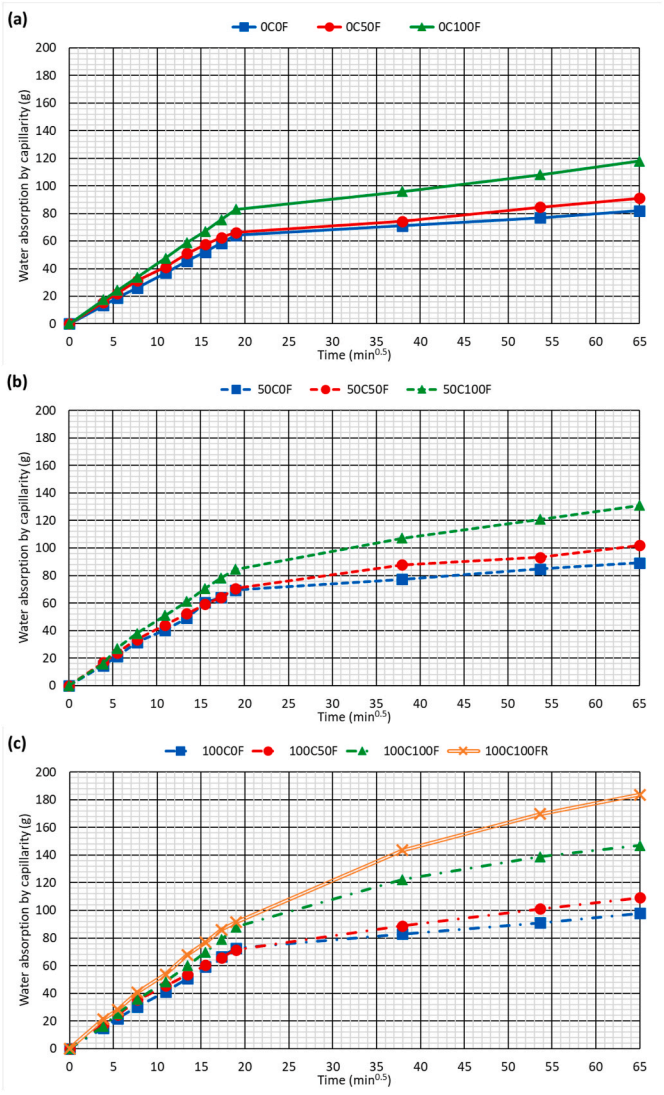

Fig. 8. Water absorption by capillarity throughout the test (72 h): (a) mixes 0C; (b) mixes 50C; (c) mixes 100C.

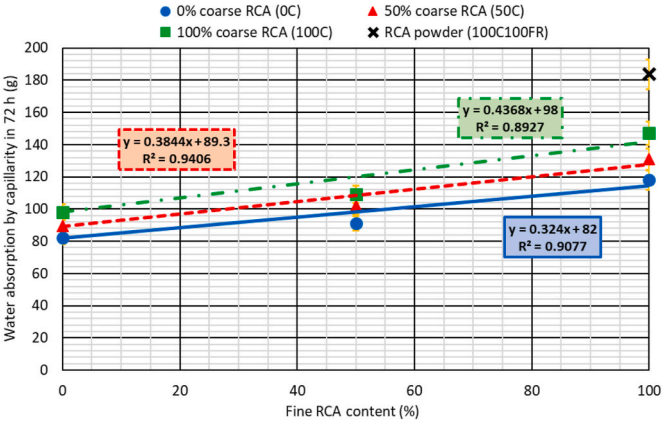

Fig. 9. Relationship between water absorption by capillarity in 72 h and fine RCA content.

worse interactions and affinity of this waste with the other concrete components [30].

In Fig. 8 and 9, the following aspects can be noted in relation to the effects of the different RCA fractions on the capillary water absorption of SCC:

- The increase in 72-h water absorption was greater when fine RCA was added (Fig. 9). Thus, the addition of 100% coarse RCA led to a 20% increase in capillary water absorption within 72 h, while the increase was 44% after having added 100% fine RCA. These results are in line with those shown in the literature, according to which the addition of the same amounts of both fine and coarse RCA generally resulted in a twofold increase in long-term water absorption compared to when only the fine fraction was used [69].
- The increase in 72-h water absorption with increased additions of fine RCA showed a linear trend, although water absorption was lower than expected with the addition of 50% fine RCA. Furthermore, the slope of the 72-h water-absorption trend line as a function of fine RCA content was greater as the coarse RCA content of the SCC was increased, as shown in Fig. 9. In the same figure, it is shown that the increased water absorption over 72 h, caused by an increasing content of coarse RCA, was similar in the SCC mixes with 0% and 50% fine RCA, but 60% higher in mixes 100 F. It can therefore be stated that there was an interaction between both RCA fractions, as confirmed by the *p*-value of interaction (0.03271) obtained with the two-way ANOVA test. As reported in other studies in relation to conventional vibrated concrete [69], increased porosity conditioned water absorption by capillarity, and was increased still further when the content of both RCA fractions were simultaneously increased; their combined effect exceeding the sum of the effect of using each RCA fraction individually [29].
- The effect of both RCA fractions was perceptible 6 h after the start of the test. As can be seen in Fig. 8, the mixtures with 0% and 50% fine RCA and the same coarse RCA content presented very similar water absorption levels during the initial 6 h of testing, with only one notable difference in this period of time when adding 100% fine RCA. The same occurred when adding coarse RCA, as the SCC with the same fine RCA content and different coarse RCA contents showed no notable difference at the start of the test. Therefore, the really comparable values were those at 6 h after the start of the test (Fig. 9) [53,70], on which the statements of the two previous bullet points are based.
- The 0–1 mm powder size fraction of this residue had the most unfavorable effect, in line with the mechanical behavior, as demonstrated by mix 100C100FR. Its addition doubled the increase in water absorption caused by adding 100% fine RCA 0–4 mm and its use is therefore not recommendable.

3.3.2. Permeation coefficient and sorptivity

There are basically two mathematical equations used to model the capillary water absorption of concrete. Each model provides a parameter that defines the rate at which the concrete absorbs water by capillary action. Both parameters are important in terms of durability, as they show how easily dangerous external agents can penetrate into concrete [10].

- On the one hand, the Fangerlund model [70], which assumes that water absorption by capillarity of concrete is a linear function of the square root of time. The slope of the aforementioned straight line expressed per unit area, so that this coefficient is not influenced by the size of the test specimen, is called the permeation coefficient, *K*, expressed in g/(m^2·min$^{0.5}$). This coefficient is calculated by Equation (1), in which ΔM is the increased mass of the specimen due to the absorption of water by capillarity in g; *A*, the exposed area in m^2; and *t*, the time in minutes. The most representative straight section of the graph of the test results must be considered for calculating this coefficient (Fig. 8), *i.e.*, the time period from 6 h to 72 h when the results of the test are fully comparable [53,70], as was explained in the previous section.

$$K = \frac{\Delta M}{A \times \Delta\sqrt{t}} \quad (1)$$

- On the other hand, the Hall model is based on the assumption that water absorption by capillarity is adjusted by a combination of functions dependent on the first power of time and the square root of time [71], as shown in Equation (2). In this expression, ΔM_u is the increase in mass due to water absorption by capillarity in g/m^2; *t*, the time in minutes; *S*, the sorptivity in g/(m^2·min$^{0.5}$); and *A* and *B*, adjustment coefficients. Sorptivity can be calculated by fitting this model to the experimental results obtained through multiple regression [44]. Sorptivity is therefore more complicated to determine than the permeation coefficient.

$$\Delta M_u = A + S \times \sqrt{t} - B \times t \quad (2)$$

Both the permeation coefficient, *K*, and the sorptivity, *S*, of each mixture are shown in Table 5. It can be observed that the higher the water absorption during the test (Fig. 8 and 9), the higher the value of these coefficients. Higher water-absorption levels are not only linked to an increase in porosity, but also to a larger pore size and higher inter-pore connectivity, so that water can penetrate faster [14,72], increasing the water-absorption-rate values [71]. Therefore, the higher the RCA content of SCC, the higher the capillary-water-absorption rate, as is also reported in the literature [8].

Sorptivity was notably higher than the permeation coefficient because the calculation of this last coefficient gives no consideration to the first 6 h of the test. For the same reason, the permeation coefficient had a higher relative increase than sorptivity following the additions of RCA. The increase of both coefficients was much greater when adding fine RCA, due to the greater increase in water absorption caused by this RCA fraction [36]. Considering the percentages of added RCA, it can be observed that in a mixture with a certain content of coarse RCA (0%, 50% or 100%), the addition of 50% fine RCA resulted in a small increase in the permeation coefficient and sorptivity compared to the increase caused by the addition of 100% fine RCA (Table 5). Similarly, in the SCC mixes with a certain fine RCA content, the addition of 50% coarse RCA resulted in a smaller increase in both coefficients than adding 100% coarse RCA. These effects have also been observed when adding aggregates of similar nature in vibrated concrete [71] and may be explained by the interactions between both RCA fractions regarding water absorption by capillarity explained in the previous section. Finally, in spite of all the above, the coefficients of mix 100C100FR, manufactured with RCA powder, were the highest, probably due to the larger size of its pores, in which the water could penetrate faster [65].

Concrete durability may be analyzed with these coefficients [1,9]. In general, for instance, permeation coefficients lower than 35

Table 5
Permeation coefficient, K; sorptivity, S; and accessible porosity of the mixes.

Mix	Permeation coefficient *K* (g/m^2·min$^{0.5}$)	Sorptivity *S* (g/m^2·min$^{0.5}$)	R^2 Hall model adjustment (%)	Accessible porosity (%)
0C0F	38.1	2617	94.85	8.2
0C50F	53.0	2669	94.44	9.1
0C100F	75.1	3354	96.07	11.8
50C0F	42.6	2731	94.62	8.9
50C50F	67.0	2767	97.06	10.2
50C100F	99.5	3582	97.65	13.1
100C0F	54.1	2923	95.70	9.8
100C50F	80.9	2965	97.35	10.9
100C100F	126.3	3882	99.25	14.7
100C100FR	197.2	4149	99.81	18.4

g/(m^2·min$^{0.5}$) correspond to high-quality concrete mixtures; if the value exceeds 100 g/(m^2·min$^{0.5}$), the quality of concrete is qualified as poor, due to the risk of easy penetration of external harmful agents, such as sulphates and chlorides [10]. The results obtained were in line with the values of similar studies in the literature [29], so that all the mixtures presented an intermediate durable quality, with a permeation coefficient between 35 and 100 g/(m^2·min$^{0.5}$). Only mixes 100C100F and 100C100FR might present durability problems (poor durable quality, permeation coefficient higher than 100 g/(m^2·min$^{0.5}$)), due to the accessibility of aggressive external agents [18].

3.3.3. Effective (accessible) porosity

Water absorption by capillarity over 72 h, a quick and easily performed test, provides a coarse estimation of the effective (accessible) porosity of concrete [8]. According to both the Fangerlund and the Hall models [70,71], the porosity of the mixtures can be calculated according to Equation (3), in which ε_e is the accessible porosity (interconnected pores) of the mixture as a percentage (%); ΔM, the total mass increase over the 72 h of the specimen, due to water absorption by capillarity in g; V, the volume of the specimen in cm^3; and ρ, the water density (1 g/cm^3).

$$\varepsilon_e = \frac{\Delta M}{V \times \rho} \times 100 \tag{3}$$

The effective porosity values are shown in the fourth column of Table 5. As expected, the results were in accordance with the water absorption and water-absorption-rate coefficients [70,71]. Thus, the fine RCA caused a greater increase in porosity than the coarse RCA, as the reference mix (0C0F)) presented an effective porosity of 8.2%, and mixes 100C0F and 0C100F of 9.8% and 11.8%, respectively. Moreover, porosity following the addition of 50% of any RCA fraction increased less than expected according to the effective porosity when adding 100%. Behavior that reflects the aforementioned interaction between both RCA fractions.

3.3.4. Effective porosity estimation

The porosity of concrete prepared with NA is linked to the amount of free (effective) water, *i.e.*, the water that is not absorbed by the aggregate of the concrete mix [5,10]. In case alternative materials, such as RCA, are added, the affinity between them and the rest of the concrete components also conditions this property [35]. Therefore, both aspects have to be considered in any estimation of concrete porosity.

The effective w/c ratio remained constant in the SCC mixes of this study, for the calculation of which the water absorption within 15 min (mixing time) of the aggregates was considered (Table 1). This implied that, since all the mixes had the same amount of cement, the free water after 15 min of mixing was the same in all the mixes. Nevertheless, the porosity was completely different in all of them (Table 5), which reveals the relevance of the affinity between the different concrete components. It is therefore necessary to look for a variable that shows the influence of the water added to the mixture and, indirectly, the aforementioned affinity.

After different attempts, it was found that the effective water at 24 h, which has no real physical meaning, since at 24 h the concrete has already hardened, fulfilled both requirements. On the one hand, it reflected the variation of the amount of water added to the SCC when incorporating RCA to maintain the workability [45]. On the other, the large difference in 24-h water absorption between NA and RCA and between both RCA fractions [48] proved to be a variable that statistically reflected the affinity of RCA with the other SCC components. This magnitude can be calculated according to Equation (4), in which EW_{24} is the 24-h effective water in kg/m^3; W, the water added to the concrete in kg/m^3; $WA_{24,i}$, the 24-h water absorption of each aggregate in percentage; and AA_i, the added amount of each aggregate in kg/m^3.

$$EW_{24} = W - \sum_i \left(\frac{WA_{24,\,i}}{100} \times AA_i \right) \tag{4}$$

The performance of a simple regression between the 24-h effective water (EW_{24}, kg/m^3) and the effective porosity (P, %) showed that both magnitudes were related to each other with a double reciprocal model and a high coefficient R^2 (95.36%). This model, shown in Equation (5) and depicted in Fig. 10a, was used to estimate the effective porosity of the mixtures with a maximum deviation of 15% with respect to the experimental value, as shown in Fig. 10b.

$$P = \frac{1}{0.44 - \frac{48.04}{EW_{24}}} \tag{5}$$

The porosity of concrete is undoubtedly linked to its composition, as has been clearly shown in this section. In addition to the inclusion of alternative materials, porosity is likewise conditioned by the cement content, the aggregate-to-cement ratio, and the type and amount of admixture in use [14,18]. The model presented in Equation (5) is therefore only valid for an SCC of a similar composition to the one in this research work, which has standard amounts of all components, *i.e.*, the SCC concrete developed in this study can be considered conventional. A statistical adjustment of results of different mix compositions and workability types (vibrated, pumpable, and self-compacting) will be needed to formulate a more generic expression.

3.4. Estimation of mechanical properties through porosity

Different studies in the literature have reported models for estimating the mechanical properties of concrete with RCA [31,44,73]. These models generally vary depending on the fraction of RCA that is added. In this section, the aim is to show the usefulness of porosity for estimating the mechanical properties of concrete, whatever the combination of the RCA fraction in use. In addition, models for estimating the mechanical behavior of conventional SCC are also provided.

3.4.1. Simple regression

Table 6 shows the simple-regression models that allow the most accurate estimation of the mechanical properties of the mixtures as a function of their porosity (P, in percent %). In addition, the expressions that provide the minimum expected value of each mechanical property at a confidence level of 95% are also included. Maximization of the coefficient R^2 was performed to obtain all these expressions.

It can be observed that the optimal relationship between porosity and those mechanical properties that depend on the application of a single type of stress -compression (compressive strength and modulus of elasticity) or tensile (splitting tensile strength)- was always of the same nature. In other words, the adjustment model always corresponded to the expression of Equation (6) (MP, mechanical property; P, porosity), while only the adjustment coefficients a and b varied. It was also reflected in the expression for the determination of the minimum expected value of the different mechanical properties, since this expression always responded to Equation (7) (MP^{min}, minimum expected value of the mechanical property; P, porosity), once again varying only the adjustment coefficients, a and b. The flexural strength, which depends on the compressive and tensile behavior of the concrete, presented expressions of a different nature.

$$MP = \frac{1}{a + b \times P^2} \tag{6}$$

$$MP^{min} = exp\left(a - b \times \sqrt{P}\right) \tag{7}$$

Fig. 11 shows the comparison between the experimental values of all the mechanical properties and the value predicted with the models listed in Table 6. For each experimental value, four values were calculated using these models: the mechanical property estimated with the

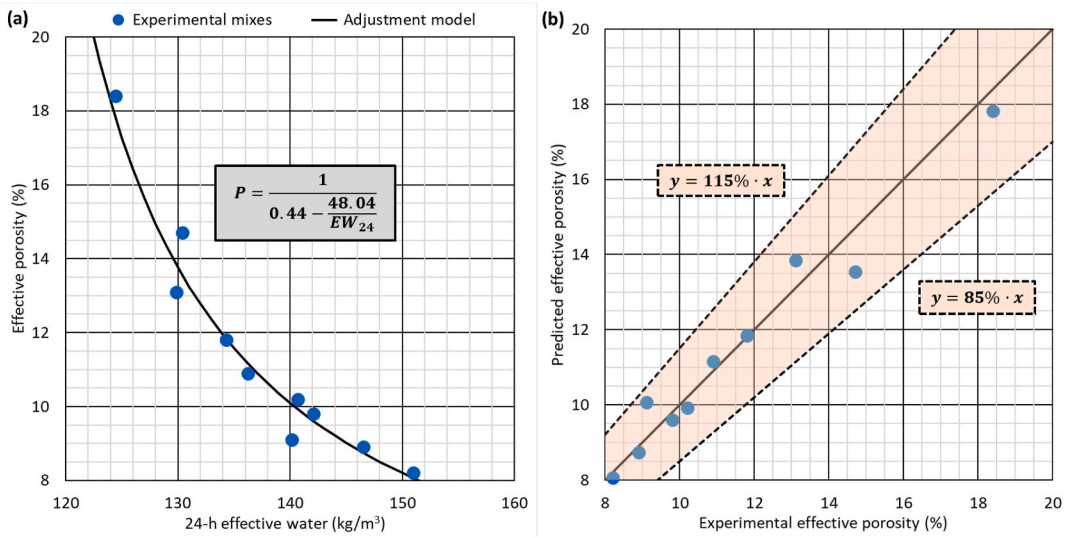

Fig. 10. (a) Simple-regression model between 24-h effective water and effective porosity; (b) Relationship between experimental and predicted effective porosity.

Table 6
Simple-regression models between porosity and mechanical properties.

Property	Simple-regression adjustment model	Minimum expected value formula	Coefficient R^2 (%)
Compressive strength at 7 days (CS_7, MPa)	$CS_7 = 1/(0.00564 + 0.00018 \times P^2)$	$CS_7^{min} = exp(6.11 - 0.81 \times \sqrt{P})$	97.78
Compressive strength at 28 days (CS_{28}, MPa)	$CS_{28} = 1/(0.012220 + 0.000093 \times P^2)$	$CS_{28}^{min} = exp(5.57 - 0.58 \times \sqrt{P})$	95.44
Modulus of elasticity at 7 days (ME_7, GPa)	$ME_7 = 1/(0.01790 + 0.00015 \times P^2)$	$ME_7^{min} = exp(5.36 - 0.63 \times \sqrt{P})$	97.24
Modulus of elasticity at 28 days (ME_{28}, GPa)	$ME_{28} = 1/(0.01731 + 0.00013 \times P^2)$	$ME_{28}^{min} = exp(5.35 - 0.60 \times \sqrt{P})$	96.82
Splitting tensile strength at 28 days (STS_{28}, MPa)	$STS_{28} = 1/(0.1532 + 0.0012 \times P^2)$	$STS_{28}^{min} = exp(2.94 - 0.56 \times \sqrt{P})$	97.16
Flexural strength at 28 days (FS_{28}, MPa)	$FS_{28} = 7.288 - 0.017 \times P^2$	$FS_{28}^{min} = 6.770 - 0.018 \times P^2$	96.16

experimental porosity value, the mechanical property estimated from the porosity calculated using the 24-h effective water value (Equation (5)), the minimum value of the mechanical property calculated using the experimentally determined porosity value, and the minimum value of the mechanical property obtained from the estimated porosity value (Equation (5)). The accuracy of the model can be seen in its estimates of the mechanical behavior of SCC, because of the following reasons, which also underline the usefulness of the porosity values estimated with Equation (5):

- Regardless of the porosity value under consideration, whether experimental or estimated, the estimated value of the mechanical property never varied by more than ±20% from the experimental value, which is a reasonable level of accuracy. Only the flexural strength of mix 100C100FR (Fig. 11f) never met this aspect, due to the remarkably low experimental value (1.15 MPa).
- In general, the estimated value of the mechanical property was lower than the experimental value. This situation occurred more frequently when the experimentally measured porosity values were used. It shows that in most cases the proposed models never overestimated the mechanical property. When the mechanical property was overestimated, this overestimation was on average lower than 15%. The values obtained with these models could therefore be safely used in structural design [50,74].
- Obviously, the minimum expected value was always lower than the predicted one and provided an adequate safety margin in all cases. But in addition, the minimum expected value was always lower than the experimental value except in 5 out of 60 tests (8%). Therefore, the minimum expected value can be considered an adequate estimation of the mechanical property from a safety-theory approach [50,74]. This trend was found regardless of considering the experimental or the estimated porosity.

3.4.2. *Multiple regression*

The estimation of the mechanical properties of SCC with RCA through porosity levels can be performed reliably and safely, as shown in the previous section. However, the porosity of the mixtures must be correctly determined or an accurate equation for its estimation must be established, such as the one obtained in this study (Equation (5)). Either incorrect moisture conditioning of the test specimens or over- or underestimation of the water layer height when performing the capillary-water-absorption test could lead to incorrect porosity values [1,9]. It implies that the application of the simple-regression models (Table 6) might result in an incorrect estimation of the mechanical properties of the SCC, despite their high accuracy. One way of avoiding this problem is to complement porosity with another property of the concrete, so that multiple-regression models may be used to estimate the mechanical properties. In this way, even if the value of porosity is incorrect, the error in the estimation of the mechanical property will be much smaller, because the second prediction variable will help to maintain predictive accuracy [44].

Compressive strength is the most commonly and easily measured mechanical property in commercially produced concrete [37]. In addition, it has often been related to other mechanical properties, as shown by the formulas contained in international standards such as Eurocode 2 [50] and ACI-318 [74]. For these reasons, it was decided to develop multiple-regression models in which the estimation of the SCC mechanical properties was based on the porosity and compressive strength of the mixtures. This approach follows the traditional trend and provides greater robustness to the estimation of the mechanical behavior of SCC based on porosity, while disregarding the RCA fraction and amount in use. Simple-regression models with compressive strength as the only

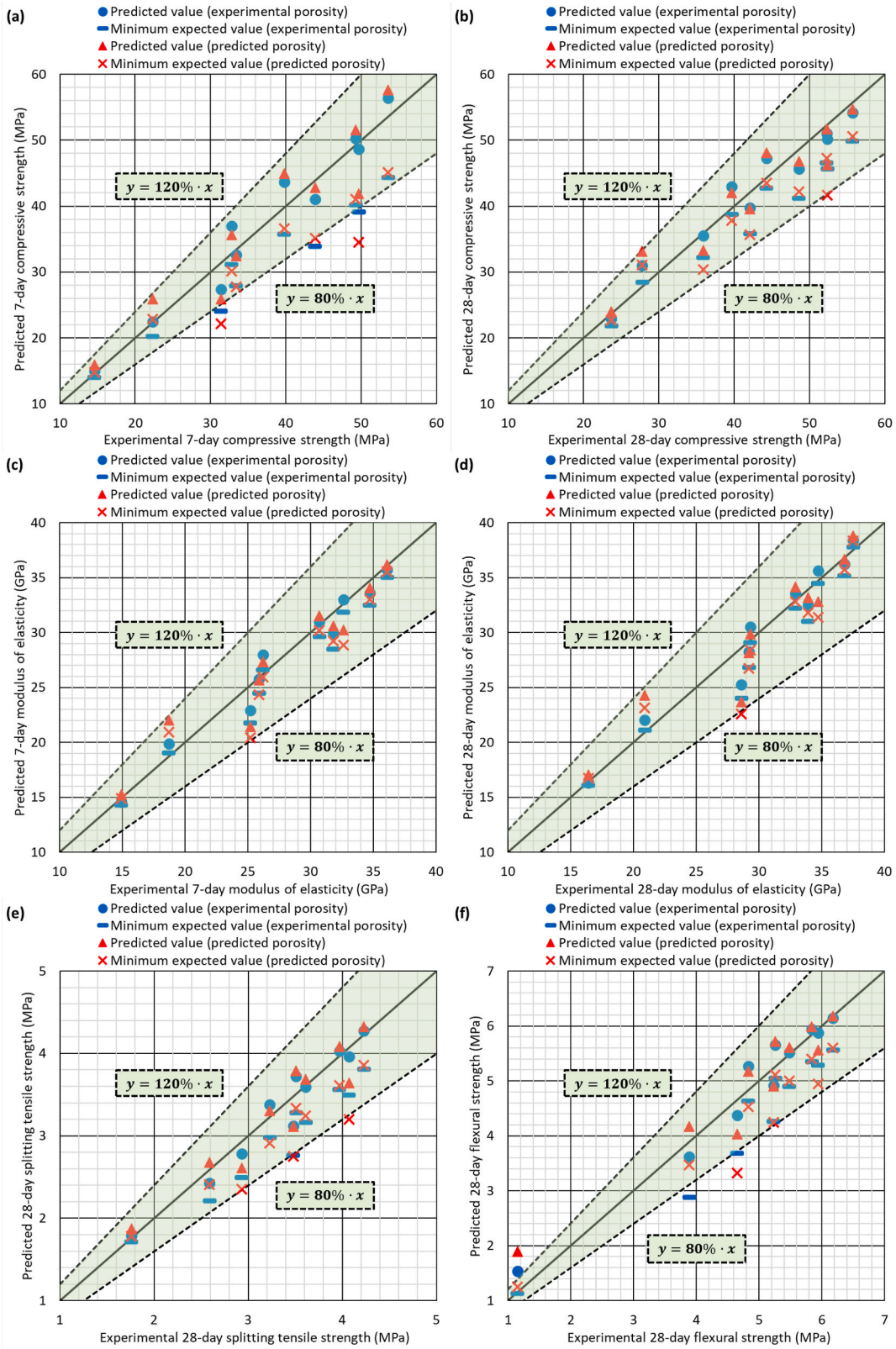

Fig. 11. Comparison between experimental and predicted mechanical properties using simple-regression models: (a) 7-day compressive strength; (b) 28-day compressive strength; (c) 7-day modulus of elasticity; (d) 28-day modulus of elasticity; (e) 28-day splitting tensile strength; (f) 28-day flexural strength.

prediction variable have been shown to depend on the RCA fraction used to produce the concrete [31,73]. However, using multiple-regression models implies that the estimation of compressive strength can only be performed through simple-regression models (Table 6).

The development of simple-regression modeling of the different mechanical properties set against the compressive strength values showed that the relation between the modulus of elasticity and splitting tensile strength could be optimally adjusted, by RCA fractions, to

Equation (8) (*MP*, mechanical property, modulus of elasticity and splitting tensile strength; *CS*, compressive strength), varying only the adjustment coefficients (*a* and *b*). Therefore, the trend shown by the simple regression between these properties and porosity was maintained, in which the optimal model was always similar for those mechanical properties that depended on a single type of stress. Likewise, the optimal simple-regression model by RCA fractions for flexural strength presented a different expression (Equation (9); *FS*, flexural strength).

$$MP = (a + b \times ln(CS))^2 \quad (8)$$

$$FS = \sqrt{a + b \times ln(CS)} \quad (9)$$

By combining the expressions of the simple-regression models between porosity and mechanical properties, and between compressive strength and mechanical properties, the models shown in Table 7 (*P*, porosity in %; CS_7, 7-day compressive strength in MPa; CS_{28}, 28-day compressive strength in MPa; *CS*, compressive strength regardless of age) were obtained. It can be observed that the R^2 coefficients of all the models were very high, in all cases over 96%, reflecting the accuracy of the models under development. Furthermore, in Table 8, the formulas to calculate the minimum expected value at a confidence level of 95% through multiple regression are shown. The formulas for calculating the minimum expected value were of the same nature (same mathematical expression but with different adjustment coefficients) as the estimation models (Table 7).

Fig. 12 shows the comparison between the experimental value of the different mechanical properties and the value estimated through the multiple-regression models. Furthermore, the minimum expected value is also shown. The following three aspects should therefore be emphasized:

- The multiple-regression model estimations, with deviation values of ±10% with respect to the experimental value, were much more accurate than the results of the simple-regression models. The flexural strength of mix 100C100FR never met this requirement, due to the very low experimental value obtained. However, the greater complexity of the multiple-regression models is not in their favor, making their application slightly more difficult than that of the simple-regression models [44].
- The estimation was equally correct regardless of whether the experimentally measured porosity or the porosity estimated through Equation (5) was used. In fact, the values of the mechanical properties calculated with each porosity reading differed between each other by 5% on average, lower than the 12% of the simple-regression models (Fig. 11). An accuracy level that was due to the introduction of compressive strength as a second variable, which reduced the estimation dependence on porosity.
- The minimum expected value of the mechanical properties was always lower than the experimental one, regardless of the porosity levels, whether experimentally measured or predicted. Therefore, the use of the minimum expected value was always on the safe side.

Table 7
Multiple-regression models between porosity, compressive strength and mechanical properties.

Property	Multiple-regression adjustment model	Coefficient R^2 (%)
7-day modulus of elasticity (ME_7, in GPa)	$ME_7 = \frac{(1.0984 + 3.0593 \times ln(CS_7))^2}{4.6140 + 0.0049 \times P^2}$	98.54
28-day modulus of elasticity (ME_{28}, in GPa)	$ME_{28} = \frac{(-0.12354 + 0.85469 \times ln(CS_{28}))^2}{0.26555 + 0.00036 \times P^2}$	97.78
Modulus of elasticity regardless of age (*ME*, in GPa)	$ME = \frac{(0.45129 + 0.94915 \times ln(CS))^2}{0.44396 + 0.00069 \times P^2}$	97.75
28-day splitting tensile strength (STS_{28}, in MPa)	$STS_{28} = \frac{(0.233 + 1.645 \times ln(CS_{28}))^2}{10.094 + 0.016 \times P^2}$	97.58
28-day flexural strength (FS_{28}, in MPa)	$FS_{28} = (\sqrt{93.5503 - 10.2686 \times ln(CS_{28})}) \times (1.0015 - 0.0024 \times P^2)$	96.35

Table 8
Multiple-regression models between porosity, compressive strength, and mechanical properties.

Property	Minimum expected value formula
7-day modulus of elasticity (ME_7, in GPa)	$ME_7 = \frac{(-0.31912 + 0.85140 \times ln(CS_7))^2}{0.26860 + 0.00026 \times P^2}$
28-day modulus of elasticity (ME_{28}, in GPa)	$ME_{28} = \frac{(-0.43389 + 0.72480 \times ln(CS_{28}))^2}{0.15811 + 0.00029 \times P^2}$
Modulus of elasticity regardless of age (*ME*, in GPa)	$ME = \frac{(-0.00052 + 0.66913 \times ln(CS))^2}{0.18546 + 0.00033 \times P^2}$
28-day splitting tensile strength (STS_{28}, in MPa)	$STS_{28} = \frac{(-0.0778 + 0.8970 \times ln(CS_{28}))^2}{2.7811 + 0.0070 \times P^2}$
28-day flexural strength (FS_{28}, in MPa)	$FS_{28} = (\sqrt{75.7772 - 5.5062 \times ln(CS_{28})}) \times (0.8931 - 0.0024 \times P^2)$

Underlining the greater robustness of prediction of the multiple-regression models regarding the porosity value compared to simple-regression models, Fig. 13 shows the comparison between the experimental value and the value predicted by both types of models from an experimental porosity that was both underestimated and overestimated by 30%. The value estimated by the multiple-regression models only deviated from the experimental value by 15% on average, a very similar value to the deviation obtained with the correct porosity value, which was 10% (Fig. 12). However, the values estimated by the simple-regression models deviated from the experimental values by 40% on average, while this deviation was only 20% when using the correct value of porosity. It is therefore evident that an incorrect determination of porosity had a lower impact on the predictive accuracy of the multiple-regression models, due to the introduction of compressive strength as a second predictive variable [44]. Both variables had a very similar influence on the prediction of each mechanical property, hence the use of multiple-regression models statistically halved the estimation errors due to an incorrectly determined porosity value.

3.4.3. Validation of the models

Fig. 13 can be seen as an initial validation of the models that were developed. This figure shows that the estimation of the mechanical properties through these models was correctly performed, even if there was a variation of the porosity, especially through the multiple-regression models. However, to guarantee the usefulness and reliability of the models, Fig. 14 shows the comparison between the experimental value and the value estimated through the multiple-regression models of the 28-day mechanical properties collected in different studies of the literature [18,66,75–79]. This validation was only performed with the multiple-regression models because they were determined with the expressions from the simple-regression models and because their use is recommended, as indicated in the previous section.

The studies consulted [18,66,75–79] for the results validation analyses reported the mechanical behavior of conventional compositions of SCC manufactured with RCA, in line with the mixes from this research. Therefore, all the mixes used in the validation presented cement contents between 300 and 350 kg/m^3, and effective w/c ratios between 0.45 and 0.50. In addition, all of them incorporated 0–100% RCA in the coarse fraction, in the fine fraction, or in both. At the time of mixing, the RCA waste had always been stored for use under outdoor ambient conditions, as is standard practice [29]. In addition, the mixing process in all cases lasted between 5 and 15 min, which is the usual time for the

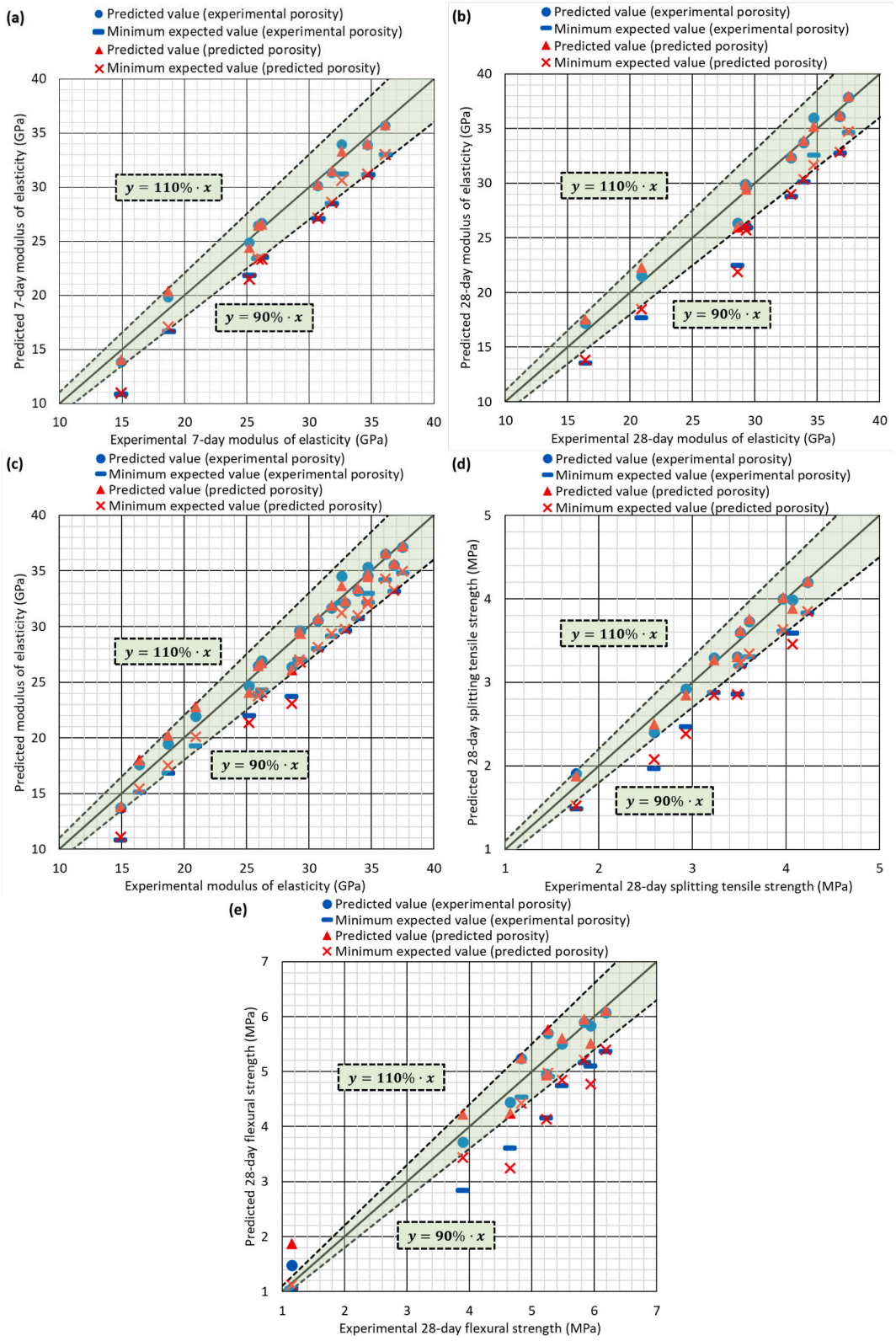

Fig. 12. Comparison between experimental and predicted mechanical properties through multiple-regression models: (a) 7-day modulus of elasticity; (b) 28-day modulus of elasticity; (c) modulus of elasticity regardless of age; (d) 28-day splitting tensile strength; (e) 28-day flexural strength.

manufacture of concrete with RCA [52]. In all the validation mixtures, the capillary-water-absorption test results determined porosity.

As expected, the estimated mechanical properties of SCC from other studies were less accurate than the properties estimated in this study for the concrete mixes manufactured, with which the models were developed. However, at a 95% confidence level, the estimated values only deviated by ±20% from the experimental ones. This limit is usually considered adequate when predicting the mechanical properties of concrete, due to its high variability [80]. It can therefore be affirmed that these models can yield adequate and safe values, regardless of

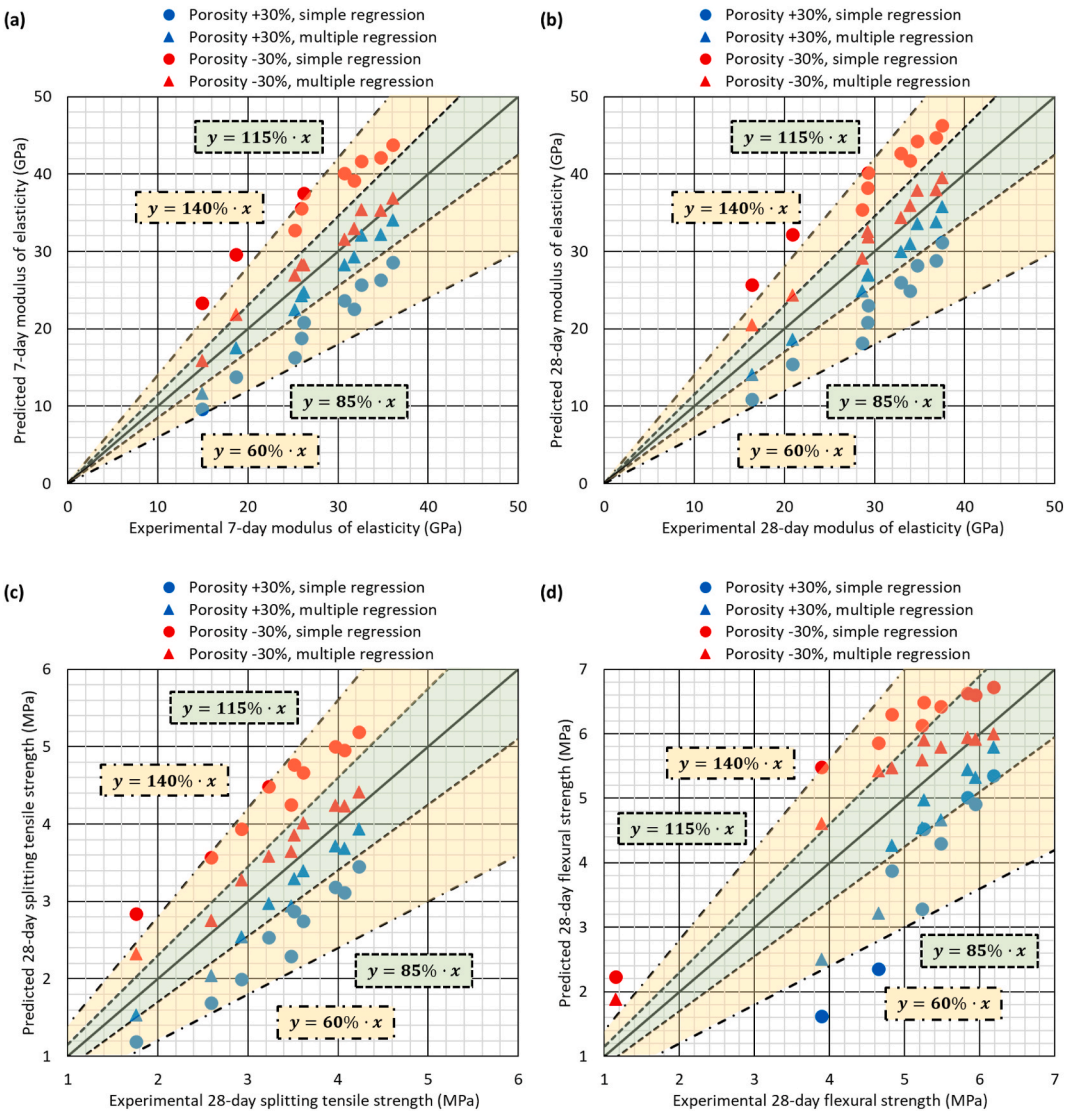

Fig. 13. Effect of varying ±30% the experimental porosity on the estimation of the mechanical properties through simple-regression and multiple-regression models: (a) 7-day modulus of elasticity; (b) 28-day modulus of elasticity; (c) 28-day splitting tensile strength; (d) 28-day flexural strength.

whether the experimentally measured porosity or the porosity estimated by Equation (5) is used for the prediction of the mechanical properties. On the other hand, the minimum expected values were lower than the experimental ones from most tests. The use of the minimum expected value was always adequate, ensuring the reliability and safety of these values for structural design.

4. Conclusions

Throughout this study, the mechanical behavior (compressive strength, modulus of elasticity, splitting tensile strength and flexural strength) and the effective porosity (capillary-water-absorption test) of a Self-Compacting Concrete (SCC) made with 0%, 50% or 100% of coarse and/or fine Recycled Concrete Aggregate (RCA) have been evaluated and likewise, the effect of the addition of RCA powder 0–1 mm. The following conclusions can be drawn in relation to these properties and behavior:

- The addition of any RCA fraction worsened all mechanical properties. Fine RCA had a more unfavorable effect than coarse RCA, although RCA powder was the most detrimental. No interaction was detected between the effect of each RCA fraction on compressive strength, modulus of elasticity, and flexural strength. There was only an interaction in splitting tensile strength, due to the increased adhesion problems between the aggregate and the cementitious matrix when fine RCA was added to the SCC that already contained coarse RCA. Therefore, in general, the weaker strength and elastic stiffness caused by the joint use of both RCA fractions was statistically equal to the sum of the decreases caused by each fraction separately.
- RCA, especially the fine fraction, increased the effective porosity and the water-absorption rate (permeation coefficient and sorptivity) of the SCC, due to the appearance of larger pore sizes with higher connectivity. Porosity could be estimated from the 24-h effective water (Equation (5)), as this variable reflected the higher porosity of SCC, due to the increase in water content when RCA was added, as well as the affinity between the components of the mix from a statistical point of view.

The great novelty of this study is the development of the porosity-based models, with which all the mechanical properties of SCC with RCA may be predicted on the basis of concrete porosity. The use of this property means the same expression may be used, regardless of the fraction of RCA that is added. Both simple-regression (Table 6) and

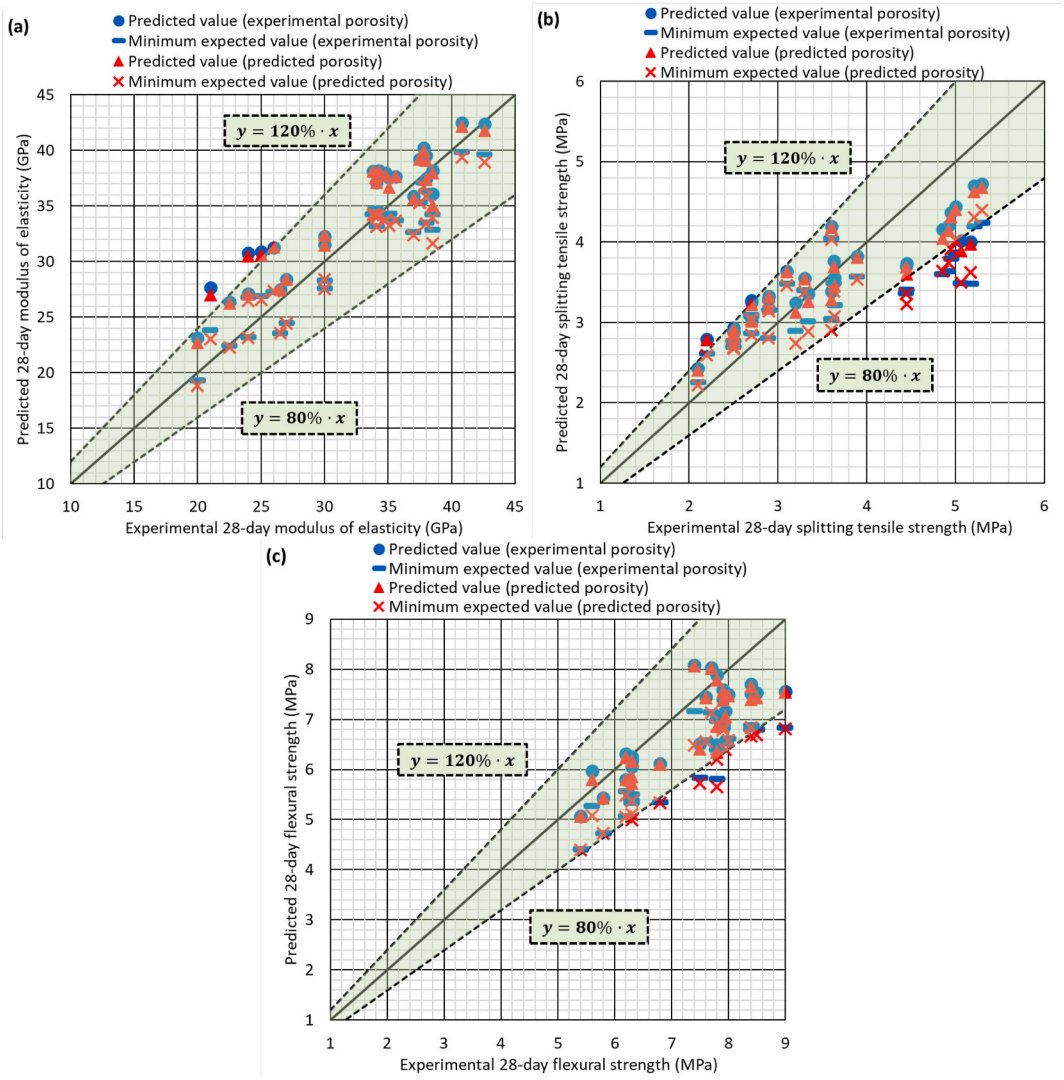

Fig. 14. Validation of multiple-regression models according to the literature [18,66,75–79]: (a) 28-day modulus of elasticity; (b) 28-day splitting tensile strength; (c) 28-day flexural strength.

multiple-regression models with compressive strength as a secondary prediction variable (Tables 7 and 8) have been provided. The accuracy and reliability of these models have been validated through some results from literature studies. The conclusions that can be drawn regarding the use of these models are as follows:

- The accuracy of the simple-regression models (±20% variation with respect to the experimental value) was lower than that of the multiple-regression models (±10% variation). Similarly, the multiple-regression model estimations of the mechanical properties, assuming porosity variations, showed greater robustness. Results that were due to the introduction of compressive strength as a secondary independent variable.
- The use of estimated porosity (Equation (5)) had no negative effects on the prediction of the mechanical properties compared to the use of experimental porosity. Therefore, the multiple-regression models developed can be used by solely experimentally determining the compressive strength, a commonly measured property in concrete in the industrial field. These models may be therefore be applied in a fast and simple way.
- The minimum expected values were lower than the experimental ones in most cases, regardless of the type of model and the porosity, experimental or predicted. Thus, their use when performing any structural design will always be appropriate, as they will never overestimate the mechanical properties.

In view of the above, the authors consider that the models provided in this study are very useful for advancing the use of RCA concrete. They would recommend the use of the capillary-water-absorption test to measure the porosity levels introduced in the models, and the use of the multiple-regression models, due to their higher accuracy and robustness. However, the models developed are only valid for SCC with conventional amounts of cement, and water in which the RCA is added under outdoor ambient conditions. Therefore, research in this field still has immense breadth and models could be developed for other types of concrete, such as vibrated concrete, and high-performance concrete. Furthermore, other SCC compositions and initial conditions of RCA could also be explored.

CRediT authorship contribution statement

Víctor Revilla-Cuesta: Conceptualization, Methodology, experimentation, Formal analysis, Data curation, Writing – original draft. **Flora Faleschini:** Methodology, Data curation, Supervision, Writing – review & editing, Project administration. **Mariano A. Zanini:** Methodology, Formal analysis, Data curation, Supervision, Writing – review &

editing. **Marta Skaf:** Conceptualization, Methodology, experimentation, Supervision, Writing – review & editing. **Vanesa Ortega-López:** Conceptualization, Supervision, Writing – review & editing, Project administration, Funding acquisition.

Declaration of competing interest

The authors declare that they have no known competing financial interests or personal relationships that could have appeared to influence the work reported in this paper.

Acknowledgements

The authors wish to express their gratitude to: Spanish Ministry of Universities within the framework of the State Program for the Promotion of Talent and its Employability in R + D + i, State Mobility Subprogram, of the State Plan for Scientific and Technical Research and Innovation 2017–2020 [PRX21/00007]; the Spanish Ministry MCI, AEI, EU and ERDF [grant numbers PID2020-113837RB-I00; 10.13039/501100011033; FPU17/03374]; the Junta de Castilla y León (Regional Government) and ERDF [grant numbers UIC-231; BU119P17]; Youth Employment Initiative (JCyL) and ESF [grant number UBU05B_1274]; and finally, the University of Burgos [grant numbers SUCONS, Y135.GI] and the University of Padova.

References

[1] V. Ortega-López, J.A. Fuente-Alonso, A. Santamaría, J.T. San-José, Á. Aragón, Durability studies on fiber-reinforced EAF slag concrete for pavements, Construct. Build. Mater. 163 (2018) 471–481, https://doi.org/10.1016/j.conbuildmat.2017.12.121.

[2] W. Soja, F. Georget, H. Maraghechi, K. Scrivener, Evolution of microstructural changes in cement paste during environmental drying, Cement Concr. Res. 134 (2020) 106093, https://doi.org/10.1016/j.cemconres.2020.106093.

[3] L. Zingg, M. Briffaut, J. Baroth, Y. Malecot, Influence of cement matrix porosity on the triaxial behaviour of concrete, Cement Concr. Res. 80 (2016) 52–59, https://doi.org/10.1016/j.cemconres.2015.10.005.

[4] A. du Plessis, W.P. Boshoff, A review of X-ray computed tomography of concrete and asphalt construction materials, Construct. Build. Mater. 199 (2019) 637–651, https://doi.org/10.1016/j.conbuildmat.2018.12.049.

[5] A. Koenig, Analysis of air voids in cementitious materials using micro X-ray computed tomography (μXCT), Construct. Build. Mater. 244 (2020) 118313, https://doi.org/10.1016/j.conbuildmat.2020.118313.

[6] P. Basu, B.S. Thomas, R. Chandra Gupta, V. Agrawal, Strength, permeation, freeze-thaw resistance, and microstructural properties of self-compacting concrete containing sandstone waste, J. Clean. Prod. 305 (2021) 127090, https://doi.org/10.1016/j.jclepro.2021.127090.

[7] M. Thiam, M. Fall, Engineering properties of a building material with melted plastic waste as the only binder, J. Build. Eng. 44 (2021) 102684, https://doi.org/10.1016/j.jobe.2021.102684.

[8] J. Nobre, M. Bravo, J. de Brito, G. Duarte, Durability performance of dry-mix shotcrete produced with coarse recycled concrete aggregates, J. Buil. Eng. 29 (2020) 101135, https://doi.org/10.1016/j.jobe.2019.101135.

[9] B. Cantero, M. Bravo, J. de Brito, I.F. Sáez del Bosque, C. Medina, Water transport and shrinkage in concrete made with ground recycled concrete-additioned cement and mixed recycled aggregate, Cement Concr. Compos. 118 (2021) 103957, https://doi.org/10.1016/j.cemconcomp.2021.103957.

[10] A. Santamaría, A. Orbe, J.T. San José, J.J. González, A study on the durability of structural concrete incorporating electric steelmaking slags, Construct. Build. Mater. 161 (2018) 94–111, https://doi.org/10.1016/j.conbuildmat.2017.11.121.

[11] G. Chen, F. Li, J. Geng, P. Jing, Z. Si, Identification, generation of autoclaved aerated concrete pore structure and simulation of its influence on thermal conductivity, Construct. Build. Mater. 294 (2021) 123572, https://doi.org/10.1016/j.conbuildmat.2021.123572.

[12] J. Mínguez, M.A. Vicente, D.C. González, Pore morphology variation under ambient curing of plain and fiber-reinforced high performance mortar at an early age, Construct. Build. Mater. 198 (2019) 718–731, https://doi.org/10.1016/j.conbuildmat.2018.12.010.

[13] R. Wang, N. Yu, Y. Li, Methods for improving the microstructure of recycled concrete aggregate: a review, Construct. Build. Mater. 242 (2020) 118164, https://doi.org/10.1016/j.conbuildmat.2020.118164.

[14] K.C. Hover, The influence of water on the performance of concrete, Construct. Build. Mater. 25 (7) (2011) 3003–3013, https://doi.org/10.1016/j.conbuildmat.2011.01.010.

[15] M. Blasone, D. Saletti, J. Baroth, P. Forquin, E. Bonnet, A. Delaplace, Ultra-high performance fibre-reinforced concrete under impact of an AP projectile: parameter identification and numerical modelling using the DFHcoh-KST coupled model, Int. J. Impact Eng. 152 (2021) 103838, https://doi.org/10.1016/j.ijimpeng.2021.103838.

[16] Y. Kurihashi, K. Kono, M. Komuro, Response characteristics of a steel fiber-reinforced porosity-free concrete beam under an impact load, Int. J. Civ. Eng. 18 (6) (2020) 673–684, https://doi.org/10.1007/s40999-020-00501-y.

[17] M.A. Vicente, J. Mínguez, D.C. González, Computed tomography scanning of the internal microstructure, crack mechanisms, and structural behavior of fiber-reinforced concrete under static and cyclic bending tests, Int. J. Fatig. 121 (2019) 9–19, https://doi.org/10.1016/j.ijfatigue.2018.11.023.

[18] F. Fiol, C. Thomas, J.M. Manso, I. López, Transport mechanisms as indicators of the durability of precast recycled concrete, Construct. Build. Mater. 269 (2021) 121263, https://doi.org/10.1016/j.conbuildmat.2020.121263.

[19] I. Pundienė, J. Pranckevičienė, M. Kligys, O. Kizinievič, The synergetic interaction of chemical admixtures on the properties of eco-friendly lightweight concrete from industrial technogenic waste, Construct. Build. Mater. 256 (2020) 119461, https://doi.org/10.1016/j.conbuildmat.2020.119461.

[20] J.T. San-José, J.M. Manso, Fiber-reinforced polymer bars embedded in a resin concrete: study of both materials and their bond behavior, Polym. Compos. 27 (3) (2006) 315–322, https://doi.org/10.1002/pc.20188.

[21] S. Zhu, C. Wu, H. Yin, Virtual experiments of particle mixing process with the sph-dem model, Materials 14 (9) (2021) 2199, https://doi.org/10.3390/ma14092199.

[22] T. Sugamata, M. Hibino, M. Ouchi, H. Okamura, Study of the particle dispersion effect of polycarboxylate-based superplasticizers, Trans. Jpn. Concr. Inst. 21 (1999) 7–14.

[23] M. Ouchi, Y. Edamatsu, K. Ozawa, H. Okamura, Simple evaluation method for interaction between coarse aggregate and mortar's particles in self-compacting concrete, Trans. Jpn. Concr. Inst. 21 (1999) 1–6.

[24] A. Santamaría, A. Orbe, M.M. Losañez, M. Skaf, V. Ortega-Lopez, J.J. González, Self-compacting concrete incorporating electric arc-furnace steelmaking slag as aggregate, Mater. Des. 115 (2017) 179–193, https://doi.org/10.1016/j.matdes.2016.11.048.

[25] M.O. Valcuende, C. Parra, J. Benlloch, Permeability, porosity and compressive strength of self-compacting concretes, Mater. Construcción 55 (280) (2005) 17–26, https://doi.org/10.3989/mc.2005.v55.i280.203.

[26] E.R. Teixeira, A. Camões, F.G. Branco, J.C. Matos, Effect of biomass fly ash on fresh and hardened properties of high volume fly ash mortars, Crystals 11 (3) (2021) 233, https://doi.org/10.3390/cryst11030233.

[27] I.O.R. Areias, C.M.F. Vieira, H.A. Colorado, G.C.G. Delaqua, S.N. Monteiro, A.R. G. Azevedo, Could city sewage sludge be directly used into clay bricks for building construction? A comprehensive case study from Brazil, J. Build. Eng. 31 (2020) 101374, https://doi.org/10.1016/j.jobe.2020.101374.

[28] G.C. Girondi Delaqua, M.T. Marvila, D. Souza, R.J. Sanchez Rodriguez, H. A. Colorado, C.M. Fontes Vieira, Evaluation of the application of macrophyte biomass Salvinia auriculata Aublet in red ceramics, J. Environ. Manag. 275 (2020) 111253, https://doi.org/10.1016/j.jenvman.2020.111253.

[29] V. Revilla-Cuesta, M. Skaf, F. Faleschini, J.M. Manso, V. Ortega-López, Self-compacting concrete manufactured with recycled concrete aggregate: an overview, J. Clean. Prod. 262 (2020) 121362, https://doi.org/10.1016/j.jclepro.2020.121362.

[30] A.R. Khan, S. Fareed, M.S. Khan, Use of recycled concrete aggregates in structural concrete, Sustain. Constr. Mater. Technol. 2 (2019).

[31] R.V. Silva, J. De Brito, R.K. Dhir, Establishing a relationship between modulus of elasticity and compressive strength of recycled aggregate concrete, J. Clean. Prod. 112 (2016) 2171–2186, https://doi.org/10.1016/j.jclepro.2015.10.064.

[32] R.V. Silva, J. De Brito, R.K. Dhir, The influence of the use of recycled aggregates on the compressive strength of concrete: a review, Eur. J. Environ. Civ. Eng. 19 (7) (2015) 825–849, https://doi.org/10.1080/19648189.2014.974831.

[33] V.W.Y. Tam, K. Wang, C.M. Tam, Assessing relationships among properties of demolished concrete, recycled aggregate and recycled aggregate concrete using regression analysis, J. Hazard Mater. 152 (2) (2008) 703–714, https://doi.org/10.1016/j.jhazmat.2007.07.061.

[34] V. Revilla-Cuesta, V. Ortega-López, M. Skaf, J.M. Manso, Effect of fine recycled concrete aggregate on the mechanical behavior of self-compacting concrete, Construct. Build. Mater. 263 (2020) 120671, https://doi.org/10.1016/j.conbuildmat.2020.120671.

[35] J. Huang, C. Zou, D. Sun, B. Yang, J. Yan, Effect of recycled fine aggregates on alkali-activated slag concrete properties, Structure 30 (2021) 89–99, https://doi.org/10.1016/j.istruc.2020.12.064.

[36] S.K. Kirthika, S.K. Singh, Durability studies on recycled fine aggregate concrete, Construct. Build. Mater. 250 (2020) 118850, https://doi.org/10.1016/j.conbuildmat.2020.118850.

[37] F. Fiol, C. Thomas, C. Muñoz, V. Ortega-López, J.M. Manso, The influence of recycled aggregates from precast elements on the mechanical properties of structural self-compacting concrete, Construct. Build. Mater. 182 (2018) 309–323, https://doi.org/10.1016/j.conbuildmat.2018.06.132.

[38] D. Carro-López, B. González-Fonteboa, J. De Brito, F. Martínez-Abella, I. González-Taboada, P. Silva, Study of the rheology of self-compacting concrete with fine recycled concrete aggregates, Construct. Build. Mater. 96 (2015) 491–501, https://doi.org/10.1016/j.conbuildmat.2015.08.091.

[39] A.S. Saha, K.M. Amanat, Rebound hammer test to predict in-situ strength of concrete using recycled concrete aggregates, brick chips and stone chips, Construct. Build. Mater. 268 (2021) 121088, https://doi.org/10.1016/j.conbuildmat.2020.121088.

[40] H. Ahmed, M. Tiznobaik, S.B. Huda, M.S. Islam, M.S. Alam, Recycled aggregate concrete from large-scale production to sustainable field application, Construct.

Build. Mater. 262 (2020) 119979, https://doi.org/10.1016/j.conbuildmat.2020.119979.
[41] J.J. Xu, W.G. Chen, C. Demartino, T.Y. Xie, Y. Yu, C.F. Fang, M. Xu, A Bayesian model updating approach applied to mechanical properties of recycled aggregate concrete under uniaxial or triaxial compression, Construct. Build. Mater. 301 (2021) 124274, https://doi.org/10.1016/j.conbuildmat.2021.124274.
[42] S.R. Salimbahrami, R. Shakeri, Experimental investigation and comparative machine-learning prediction of compressive strength of recycled aggregate concrete, Soft Comput 25 (2) (2021) 919–932, https://doi.org/10.1007/s00500-021-05571-1.
[43] X. Luo, G. Liu, Y. Zhang, T. Meng, L. Zhan, Estimation of resilient modulus of cement-treated construction and demolition waste with performance-related properties, Construct. Build. Mater. 283 (2021) 122107, https://doi.org/10.1016/j.conbuildmat.2020.122107.
[44] V. Revilla-Cuesta, M. Skaf, A.B. Espinosa, A. Santamaría, V. Ortega-López, Statistical approach for the design of structural self-compacting concrete with fine recycled concrete aggregate, Mathematics 8 (12) (2020) 2190, https://doi.org/10.3390/math8122190.
[45] S. Santos, P.R. da Silva, J. de Brito, Self-compacting concrete with recycled aggregates – a literature review, J. Build. Eng. 22 (2019) 349–371, https://doi.org/10.1016/j.jobe.2019.01.001.
[46] J. Xiao, C. Wang, T. Ding, A. Akbarnezhad, A recycled aggregate concrete high-rise building: structural performance and embodied carbon footprint, J. Clean. Prod. 199 (2018) 868–881, https://doi.org/10.1016/j.jclepro.2018.07.210.
[47] En-Euronorm, Rue de stassart, 36. Belgium-1050 Brussels, European Committee for Standardization.
[48] F. Agrela, M. Sánchez De Juan, J. Ayuso, V.L. Geraldes, J.R. Jiménez, Limiting properties in the characterisation of mixed recycled aggregates for use in the manufacture of concrete, Construct. Build. Mater. 25 (10) (2011) 3950–3955, https://doi.org/10.1016/j.conbuildmat.2011.04.027.
[49] A. Santamaría, J.J. González, M.M. Losáñez, M. Skaf, V. Ortega-López, The design of self-compacting structural mortar containing steelmaking slags as aggregate, Cement Concr. Compos. 111 (2020) 103627, https://doi.org/10.1016/j.cemconcomp.2020.103627.
[50] Ec2, Eurocode 2: Design of Concrete Structures. Part 1-1: General Rules and Rules for Buildings, CEN (European Committee for Standardization), 2010.
[51] M. Bravo, J. De Brito, J. Pontes, L. Evangelista, Mechanical performance of concrete made with aggregates from construction and demolition waste recycling plants, J. Clean. Prod. 99 (2015) 59–74, https://doi.org/10.1016/j.jclepro.2015.03.012.
[52] E. Güneyisi, M. Gesoğlu, Z. Algin, H. Yazici, Effect of surface treatment methods on the properties of self-compacting concrete with recycled aggregates, Construct. Build. Mater. 64 (2014) 172–183, https://doi.org/10.1016/j.conbuildmat.2014.04.090.
[53] Rilem, CPC 11.2, Absorption of Water by Concrete by Capillarity, 1982.
[54] F. Faleschini, C. Jiménez, M. Barra, D. Aponte, E. Vázquez, C. Pellegrino, Rheology of fresh concretes with recycled aggregates, Construct. Build. Mater. 73 (2014) 407–416, https://doi.org/10.1016/j.conbuildmat.2014.09.068.
[55] V. Revilla-Cuesta, M. Skaf, A. Santamaría, J.J. Hernández-Bagaces, V. Ortega-López, Temporal flowability evolution of slag-based self-compacting concrete with recycled concrete aggregate, J. Clean. Prod. 299 (2021) 126890, https://doi.org/10.1016/j.jclepro.2021.126890.
[56] Á. Salesa, J.Á. Pérez-Benedicto, L.M. Esteban, R. Vicente-Vas, M. Orna-Carmona, Physico-mechanical properties of multi-recycled self-compacting concrete prepared with precast concrete rejects, Construct. Build. Mater. 153 (2017) 364–373, https://doi.org/10.1016/j.conbuildmat.2017.07.087.
[57] M. Nedeljković, J. Visser, B. Šavija, S. Valcke, E. Schlangen, Use of fine recycled concrete aggregates in concrete: a critical review, J. Build. Eng. 38 (2021) 102196, https://doi.org/10.1016/j.jobe.2021.102196.
[58] M. Gesoglu, E. Güneyisi, H.Ö. Öz, I. Taha, M.T. Yasemin, Failure characteristics of self-compacting concretes made with recycled aggregates, Construct. Build. Mater. 98 (2015) 334–344, https://doi.org/10.1016/j.conbuildmat.2015.08.036.
[59] S.A. Santos, P.R. da Silva, J. de Brito, Mechanical performance evaluation of self-compacting concrete with fine and coarse recycled aggregates from the precast industry, Materials 10 (8) (2017) 904, https://doi.org/10.3390/ma10080904.
[60] B. Cantero, I.F. Sáez del Bosque, A. Matías, M.I. Sánchez de Rojas, C. Medina, Inclusion of construction and demolition waste as a coarse aggregate and a cement addition in structural concrete design, Arch. Civ. Mech. Eng. 19 (4) (2019) 1338–1352, https://doi.org/10.1016/j.acme.2019.08.004.
[61] S.T. Yildirim, C. Meyer, S. Herfellner, Effects of internal curing on the strength, drying shrinkage and freeze-thaw resistance of concrete containing recycled concrete aggregates, Construct. Build. Mater. 91 (2015) 288–296, https://doi.org/10.1016/j.conbuildmat.2015.05.045.
[62] A. Gonzalez-Corominas, M. Etxeberria, Effects of using recycled concrete aggregates on the shrinkage of high performance concrete, Construct. Build. Mater. 115 (2016) 32–41, https://doi.org/10.1016/j.conbuildmat.2016.04.031.
[63] S. Boudali, B. Abdulsalam, A.H. Rafiean, S. Poncet, A. Soliman, A. Elsafty, Influence of fine recycled concrete powder on the compressive strength of self-compacting concrete (Scc) using artificial neural network, Sustainability 13 (6) (2021) 3111, https://doi.org/10.3390/su13063111.
[64] W.C. Tang, P.C. Ryan, H.Z. Cui, W. Liao, Properties of self-compacting concrete with recycled coarse aggregate, Ann. Mater. Sci. Eng. 2016 (2016) 2761294, https://doi.org/10.1155/2016/2761294.
[65] S.C. Kou, C.S. Poon, Properties of self-compacting concrete prepared with coarse and fine recycled concrete aggregates, Cement Concr. Compos. 31 (9) (2009) 622–627, https://doi.org/10.1016/j.cemconcomp.2009.06.005.
[66] Z. Duan, A. Singh, J. Xiao, S. Hou, Combined use of recycled powder and recycled coarse aggregate derived from construction and demolition waste in self-compacting concrete, Construct. Build. Mater. 254 (2020) 119323, https://doi.org/10.1016/j.conbuildmat.2020.119323.
[67] UNE 83966, Concrete Durability. Test Methods. Conditioning of Concrete Test Pieces for the Purpose of Gas Permeability and Capilar Suction Tests, 2008.
[68] R.V. Silva, J. de Brito, R.K. Dhir, Fresh-state performance of recycled aggregate concrete: a review, Construct. Build. Mater. 178 (2018) 19–31, https://doi.org/10.1016/j.conbuildmat.2018.05.149.
[69] G. Puente de Andrade, G. de Castro Polisseni, M. Pepe, R.D. Toledo Filho, Design of structural concrete mixtures containing fine recycled concrete aggregate using packing model, Construct. Build. Mater. 252 (2020) 119091, https://doi.org/10.1016/j.conbuildmat.2020.119091.
[70] UNE 83982, Concrete Durability. Test Methods. Determination of the Capillar Suction in Hardened Concrete, Fagerlund method, 2008.
[71] B. Cantero, I.F. Sáez del Bosque, A. Matías, M.I. Sánchez de Rojas, C. Medina, Water transport mechanisms in concretes bearing mixed recycled aggregates, Cement Concr. Compos. 107 (2020) 103486, https://doi.org/10.1016/j.cemconcomp.2019.103486.
[72] P. Anaya, J. Rodríguez, C. Andrade, B. Martín-Pérez, C.L. Hombrados, Determination of wires transfer length in prestressed concrete members with different levels of corrosion, Inf. Constr. 72 (558) (2020) 1–10, https://doi.org/10.3989/ic.71428.
[73] Y. Yu, Y. Zheng, J.J. Xu, X.L. Wang, Modeling and predicting the mechanical behavior of concrete under uniaxial loading, Construct. Build. Mater. 273 (2021) 121694, https://doi.org/10.1016/j.conbuildmat.2020.121694.
[74] ACI-318-19, Building Code Requeriments for Structural Concrete, 2019.
[75] M. Abed, R. Nemes, B.A. Tayeh, Properties of self-compacting high-strength concrete containing multiple use of recycled aggregate, J. King Saud Univ. Eng. Sci. 32 (2) (2020) 108–114, https://doi.org/10.1016/j.jksues.2018.12.002.
[76] M. Omrane, M. Rabehi, Effect of natural pozzolan and recycled concrete aggregates on thermal and physico-mechanical characteristics of self-compacting concrete, Construct. Build. Mater. 247 (2020) 118576, https://doi.org/10.1016/j.conbuildmat.2020.118576.
[77] P. Rajhans, S.K. Panda, S. Nayak, Sustainability on durability of self compacting concrete from C&D waste by improving porosity and hydrated compounds: a microstructural investigation, Construct. Build. Mater. 174 (2018) 559–575, https://doi.org/10.1016/j.conbuildmat.2018.04.137.
[78] A. Sadeghi-Nik, J. Berenjian, S. Alimohammadi, O. Lotfi-Omran, A. Sadeghi-Nik, M. Karimaei, The effect of recycled concrete aggregates and metakaolin on the mechanical properties of self-compacting concrete containing nanoparticles, Iran, J. Sci. Tech. Trans. Civ. Eng. 43 (2019) 503–515, https://doi.org/10.1007/s40996-018-0182-4.
[79] K. Zitouni, A. Djerbi, A. Mebrouki, Study on the microstructure of the new paste of recycled aggregate self-compacting concrete, Materials 13 (9) (2020) 2114, https://doi.org/10.3390/ma13092114.
[80] J.C. Salcedo, M. Fortea, The influence of structural alterations on the damages of the Amatrice earthquake, Italy (2016), Inf. Constr. 72 (559) (2020) 71378, https://doi.org/10.3989/IC.71378.